Available online at www.sciencedirect.com

jmr&t Journal of Materials Research and Technology

journal homepage: www.elsevier.com/locate/jmrt

Review Article

An overview on the use of corrosion inhibitors for the corrosion control of Mg and its alloys in diverse media

Saviour A. Umoren [a,*], *Mohammed T. Abdullahi* [b], *Moses M. Solomon* [c]

[a] *Interdisciplinary Research Center for Advanced Materials, King Fahd University of Petroleum and Minerals, Dhahran 31261, Saudi Arabia*

[b] *Department of Chemistry, College of Chemicals and Materials, King Fahd University of Petroleum and Minerals, Dhahran 31261, Saudi Arabia*

[c] *Department of Chemistry, College of Science and Technology, Covenant University, Ota, Nigeria*

ARTICLE INFO

Article history:
Received 10 April 2022
Received in revised form
2 August 2022
Accepted 4 August 2022
Available online 13 August 2022

ABSTRACT

The limiting factor towards the utilization of Mg and its alloys especially in aqueous environment is their low corrosion resistance occasioned by their high chemical reactivity and high electron negative potential. The corrosion inhibitor technology is one of the effective corrosion mitigation approaches. In this review, inorganic, organic (surfactants, ionic liquids, and Schiff bases), and polymeric substances reported as corrosion inhibitors for Mg and its alloys are discussed. Smart coatings containing corrosion inhibitors for Mg and its alloys are also highlighted. The drawbacks on current researches involving

Abbreviations: SVET, Scanning vibrating electrode technique; SDBS, Sodium dodecylbenzenesulfonate; NLS, Sodium salt of N-lauroylsarcosine; NLT, N-lauroyl-N-methyltaurine; DBS, Dodecylbenzensulphonic acid; LS, Sodium lauryl sulphate; SDS, Sodium dodecyl sulphate; ILs, Ionic liquids; [BHPz][NTf2], 1-n-butyl-2-hexylpyrazole bis(trifluoromethylsulfonyl)amide; [BOPz][NTf2], 1-n-butyl-2-octylpyrazole bis(trifluoromethylsulfonyl)amide; [BDePz][NTf2], 1-n-butyl-2-decylpyrazole bis(trifluoromethylsulfonyl)amide; [BMIM][DBP], 1-butyl-3-methylimidazolium dibutylphosphate; [BPP][NTf2], Benzyl triphenyl phosphonium bis(trifluoromethylsulfonyl)amide; [EMIm][NTf2], 1-ethyl-3-methylimidazolium bis(trifluoromethylsulfonyl)amide; [HMIm][NTf2], 1-hexyl-3-methylimidazolium bis(trifluoromethylsulfonyl)amide; [DMIm][NTf2], 1-decyl-3-methylimidazolium bis(trifluoromethylsulfonyl)amide; PCTyr, Paeonol condensation tyrosine; PCPhe, Paeonol condensation phenylalanine; PCCys, Paeonol condensation cysteine; BPMDE, N′-bis (2-pyridylmethylidene)-1,2-diiminoethane; SB, Sodium benzoate; EIS, Electrochemical impedance spectroscopy; HMTA, Hexamethylenetetramine; EG, Ethylene glycol; TEOS, Tetraethoxysilane; PEO, Plasma electrolytic oxidation; DCC, Dip chemical coating; FBAs, Functional binding agents; MBI, 2- mercaptobenzimidazole; AlFu, Aluminum fumarate; AlTp, Aluminum terephthalate metal-organic framework; REACH, Registration, evaluation authority and restriction of chemicals; PARCOM, Paris commission; Dex, Dextran; ALG, Alginate; HEC, Hydroxyethyl cellulose; GA, Gum Arabic; PEC, Pectin; CHI, Chitosan; CMC, Carboxymethyl cellulose; SA, Sodium alginate; SP, Sodium phosphate; PEG, Poly(ethylene glycol); PASP, Polyaspartic acid; SEM, Scanning electron microscope; OPE, Orange peel extracts; WGHE, Walnut green husk extract; APTS-Na, Sodium aminopropyltriethoxysilicate; TPP, 5,10,15,20-Tetraphenylporphyrin; CNT, Carbon nanotube; HNT, Halloysite nanotube; PDP, Potentiodynamic polarization; 8HQ, 8-hydroxyquinoline; LDH, Layered double hydroxide; Ce(DEHP)3, Tri(bis(2-ethylhexyl)phosphate); 2,5PDC, 2,5pyridindicarboxylate; ASP, Aspartic acid; PGA, Poly-l-glutamic acid; PA, Phytic acid; MET, Methionine; PPA, Phenylphosphonic acid; MSB, Benzoic acid; MKH, 3-aminopropyltriethoxysilane; MBT, 2-mercaptobenzothiazole; MSN, Mesoporous silica nanoparticle; SNAP, Self-assembled nanophase particle.

* Corresponding author.
E-mail address: umoren@kfupm.edu.sa (S.A. Umoren).

https://doi.org/10.1016/j.jmrt.2022.08.021

Keywords:
Mg corrosion
Corrosion inhibitors
Surfactants
Ionic liquids
Polymers
Coatings

corrosion inhibitors for Mg and its alloys have been identified and the path to chart in future researches in this area recommended.

1. Introduction

The loss in the unique properties of metals as a result of it interaction with some elements in the environment, commonly referred to as corrosion has continued to be a global concern with the annual global cost put at $2.5 trillion [1]. This phenomenon has gained attention of researchers since the era of industrial outburst, and still dominate the research space with many works geared towards mitigation [2–6] since a complete stoppage of metal corrosion is impossible.

Mg is one of the world's most abundant elements. Because of its light weight and good characteristics, it is an important engineering material. It has a density of 1.74 g/cm^3 and electronegativity of 1.31 which makes it very active. It also offers a number of attractive properties, including good castability, hot formability, outstanding machinability, good electromagnetic shielding capabilities, good biocompatibility, and recyclability [7,8]. As a result, Mg and its alloys have the potential to take the place of steel and Al in a wide range of applications. They have already been used in industries such as aerospace, airplanes, automobiles, mobile electronics, biomaterials, and others [9]. The physical and chemical properties of Mg make it a metal of choice in the drive for sustainable pollution free world.

However, the deployment of Mg on a commercial scale especially in aqueous environment has suffer huge setback due to the poor corrosion resistance occasioned by its negative equilibrium potential (−2.37 V vs SHE) and the present of impurities like Fe, Ni, and Cu which profoundly affect the corrosion resistance property [10,11] through the formation of secondary phase particles that act as the preferential site for corrosion [12].

Generally, the aqueous corrosion of Mg involves the conversion of Mg to a more stable Mg^{2+} ion via electrochemical processes [13–17]. The anodic oxidation half reaction is as illustrated as:

$$Mg \rightarrow Mg^{2+} + 2e^- \quad (1)$$

Because the electrons generated in Eq. (1) must be consumed by other species so as to maintain electroneutrality, the oxidation half reaction is accompanied by the cathodic half reduction reaction. In acidic environment, the cathodic half reaction is as given in Eqs. (2) and (3) whereas the reactions in Eqs. (4) and (5) occur in the neutral and alkaline environments [18].

$$2H^+ + 2e^- \rightarrow H_2 \; E^\circ = 0 \; V_{SHE} \quad (2)$$

$$2H_2O + 2e^- \rightarrow H_2 + 2OH^- \; E^\circ = -0.83 \; V_{SHE} \quad (3)$$

$$O_2 + 4H^+ + 4e^- \rightarrow 2H_2O \; E^\circ = 1.23 \; V_{SHE} \quad (4)$$

$$O_2 + 2H_2O + 4e^- \rightarrow 4OH^- \; E^\circ = 0.4 \; V_{SHE} \quad (5)$$

The overall reaction is therefore as:

$$Mg + 2H_2O \rightarrow Mg(OH)_2 + H_2 \; E^\circ = -2.37 \; V_{SHE} \quad (6)$$

The presence of alloying elements may modify the rate of the reaction or alter the reaction steps, but the mechanism remains unchanged. Figure 1 illustrates the corrosion mechanism of Mg and Mg alloy. Corrosion occurs majorly on the matrix phase, because the matrix is considered to be the main

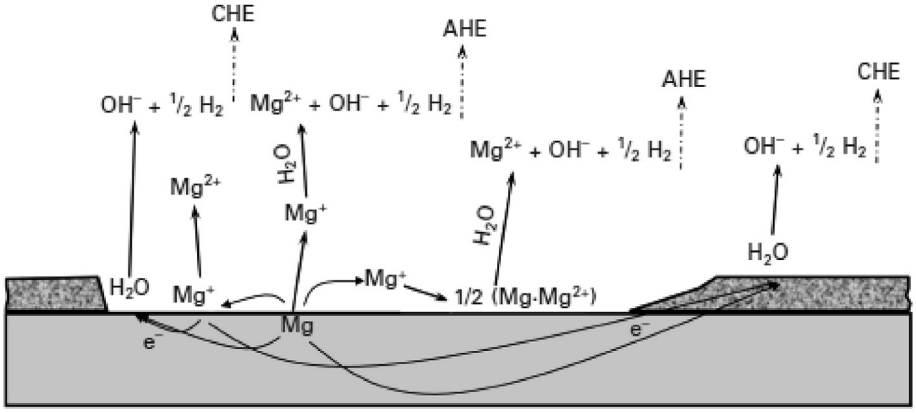

Fig. 1 – Schematic of Mg/Mg alloy corrosion mechanism.

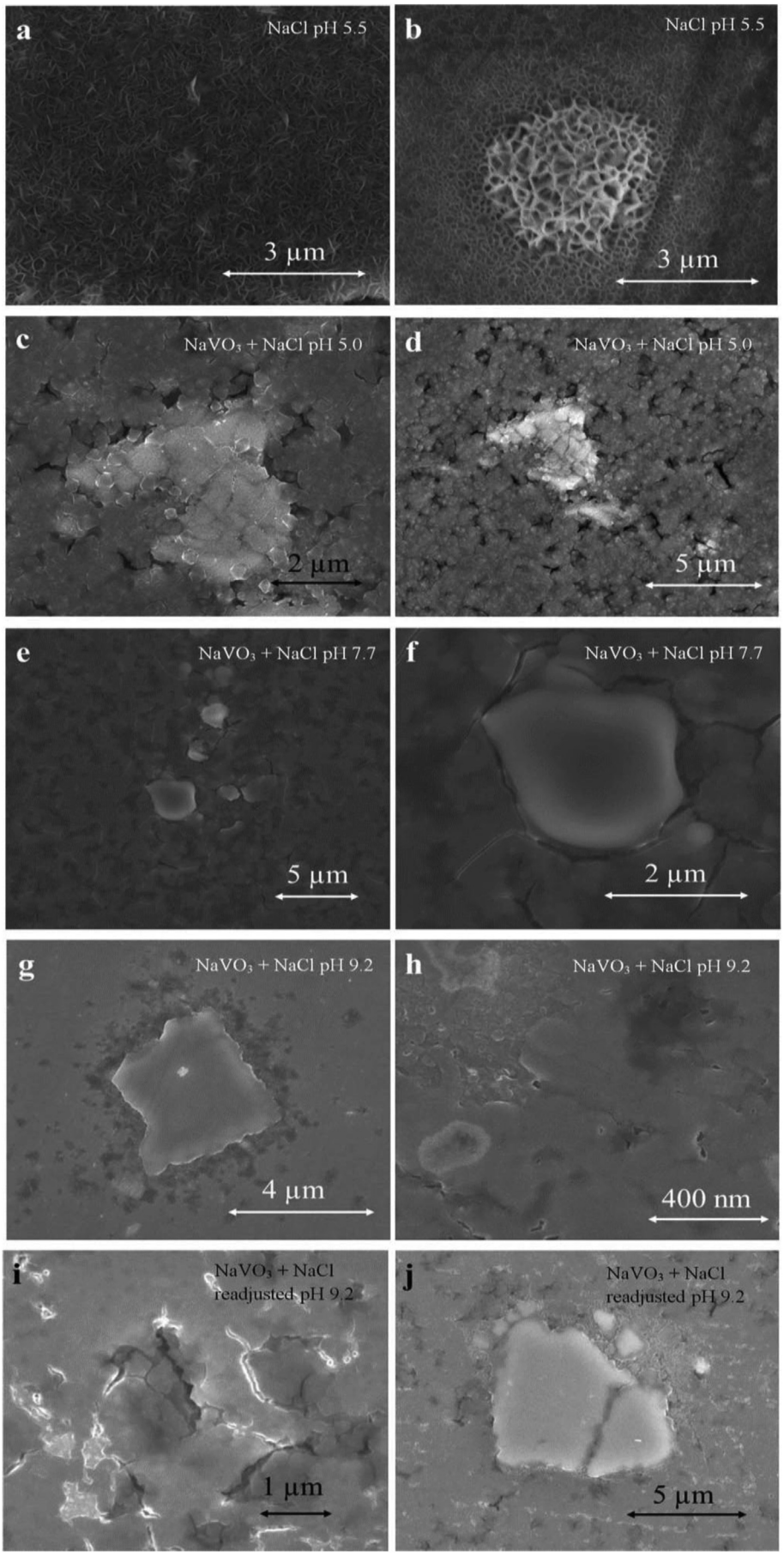
a
NaCl pH 5.5
3 μm
b
NaCl pH 5.5
3 μm
c
NaVO3 + NaCl pH 5.0
2 μm
d
NaVO3 + NaCl pH 5.0
5 μm
e
NaVO3 + NaCl pH 7.7
5 μm
f
NaVO3 + NaCl pH 7.7
2 μm
g
NaVO3 + NaCl pH 9.2
4 μm
h
NaVO3 + NaCl pH 9.2
400 nm
i
NaVO3 + NaCl
readjusted pH 9.2
1 μm
j
NaVO3 + NaCl
readjusted pH 9.2
5 μm

phase, hence the corrosion and behaviour of the matrix phase will determine the corrosion resistance of alloy. The other phases in alloy act as a barrier to either speed up or retard the corrosion process of the matrix phase.

Several techniques have been adopted to improve the corrosion resistance property of Mg. This include, alloying [19], surface coatings [20], electroless plating [21,22], and the use of corrosion inhibitors [23]. Of all these techniques, the use of corrosion inhibitor is regarded as the most simple and practical approach to control Mg and its alloys corrosion in aqueous environments. However, relative to the mitigation of Mg corrosion using coatings [24,25], it is more difficult to obtain a corrosion inhibitor especially organic corrosion inhibitor for Mg corrosion [26]. In fact, it is reported that, most compounds that effectively inhibit the corrosion of other substrates in aqueous media are ineffective for Mg and its alloys. For example, Lamaka et al. [27] screened 151 compounds (organic and inorganic) as inhibitor for Mg alloys namely AZ31, AZ91, AM50, WE43, ZE41, Elektron 21 as well as 3 grades of pure Mg in 0.5 wt.% NaCl solution. It was found that, only 15 exhibited inhibitive property and of the 15, more than 60% were compounds marked as toxic, carcinogenic, and harmful to the natural environment. Similarly, Mei et al. [28] examined the inhibitive effect of 53 organic bio-compounds (amino acids, antibiotics, vitamins, and saccharides) on CP Mg and Mg-0.8Ca alloys in chloride-rich environment and found that 80% of the tested compounds accelerated or minimally controlled the corrosion of the alloys.

Thus, this review article intends to bring into one piece information on compounds studied as corrosion inhibitors and organic coatings containing corrosion inhibitors for the control of the corrosion of Mg and Mg alloys in aqueous environments. The drawbacks in the study of corrosion inhibitor technology for Mg and its alloys are discussed and the path to chart in the future researches are suggested.

2. Corrosion inhibitors for Mg and its alloys

Mg and Mg alloys are highly reactive, hence corrode easily in aggressive environment. This reason in addition to the loose and porous corrosion products formed in the process, limit the wide application of the metal [18,29,30]. The importance attached to Mg due to its light weight and other properties has prompted wide research activities on the development of corrosion inhibitors. Corrosion inhibitors are deployed to provide corrosion protection in the transportation, power, chemical and other industries [31–33]. Inhibitors function by being physically adsorbed onto the surface of the Mg and react with metal oxide interface or other corrosive product to form insoluble materials by chemical adsorption to prevent further corrosion of the substrate.

2.1. *Inorganic corrosion inhibitors*

Inorganic inhibitors for Mg and Mg alloys corrosion are introduced to add more effective protection to the metal. The inorganic compounds investigated as inhibitors for Mg and its alloys include CeO_2 and its nanoparticles [34], SiO_2 nanoparticles [35], $Ce(NO_3)_3$, $CeCl_3$ [36], permanganate, nitrite, H_2O_2, fluoride, ZnO, molybdate and tungstate. Some of them are good passivator and this property makes them to be able to protect Mg. Examples of this type of inhibitors are chromate, nitrite, and peroxide (H_2O_2). Large amount of the inhibitor is required to effectively protect Mg and its alloys from corrosion. Because of the reaction between the compound and Mg, a layer of Mg containing products is formed that is thicker than a passive firm on the metal surface. So they are used for surface treatment of Mg alloys [37–39]. Other inorganic inhibitors like molybdate, tungstate and fluoride inhibit Mg alloys via precipitation [40–42]. Potassium fluoride (KF) is also reported as effective for the mitigation of Mg corrosion. The corrosion behaviour of Mg in ethylene glycol and it mitigation using KF was studied [40]. It was found that corrosion was significantly abated upon the addition of fluorides (1 wt.% KF) due to the reaction of F^- with Mg to form protective fluoride-containing firm on the Mg surface. Also, the salt of tungstate and molybdate inhibit the cathodic reactions of Mg alloy by forming protective layer on the cathodic active sites [41,42].

The ease at which chromate is reduced by Mg suggest its inhibitive property on the metal. Williams et al. [43] in their report detailed the strong likelihood of chromate to effectively inhibit Mg surface from attack due to the reduction of chromate to Cr^{3+} which serves as a protective film on the Mg surface.

Zhiyuan et al. [44] explored the multi-oxidative property of V and investigated the inhibitive performance of vanadate species in aqueous medium of varied pH for AZ31 Mg alloy. It was inferred that the reduction of V and adsorption is energized by the valence state of vanadium (V^{5+}, V^{4+}, V^{3+}) oxide and that the pH value of 7.7 and 9.2 supported the binding of tetrahedral species of vanadate better than the octahehedral species at acidic pH 5.0. This is possibly due to the high accommodation of exchangeable OH^- ligands [44]. Figure 2 illustrates the superior inhibition of AZ31 by the tetrahedral species at higher pH values. At pH 5.0 (Fig. 2c and d), incomplete porous film is seen on the metal surface and this could readily allow the transgression of electrolyte to the surface, the easy release of Mg^{2+} ions, and the evolution of H_2. In summary, the film provides poor corrosion inhibition. However, at pH 7.7 and 9.2 (Fig. 2e-h), dense and thick films are seen on both the matrix and secondary phase particles in the presence of tetrahedral vanadate and better inhibition is provided.

Ioannis et al. [45] evaluated the inhibitive ability of typical inorganic compounds on Mg ZK30, using electrochemical impedance spectroscopy and other techniques in NaCl solution. The inorganic compounds were calcium fluoride (CaF_2), sodium fluoride (NaF), zinc nitrate [$Zn(NO_3)_2$] and ammonium phosphate dibase $(NH_4)_2HPO_4$. In 5 mM NaCl solution, CaF_2 and $(NH_4)_2HPO_4$ were potent and inhibited Mg ZK30 corrosion while in 50 mM NaCl solution, NaF and $(NH_4)_2HPO_4$ showed protection against the corrosion of Mg ZK30. This action can

Fig. 2 – Corrosion morphology after 1 h exposure in 0.1 M NaCl (a, b), and 4 mM $NaVO_3$ at different pH (c, d at pH 5.0; e, f at pH 7.7; g, h at pH 9.2; i, j at re-adjusted pH 9.2). Reproduced from Ref. [44].

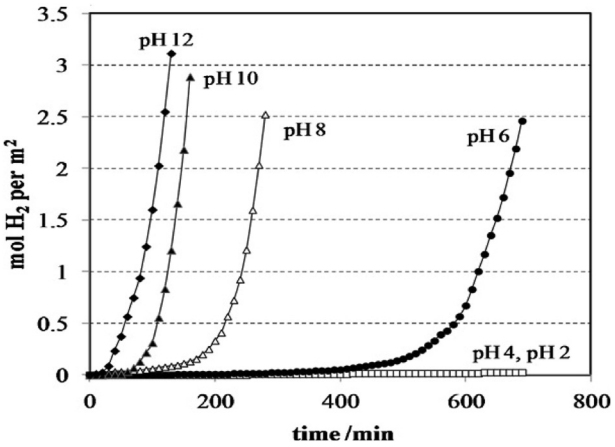

Fig. 3 – Evolution of hydrogen gas as a function of time for Mg immersed in aerated 5% (w/v) aqueous sodium chloride solution with pH adjusted to values between pH 2 and pH 12 in the presence of 0.01 mol dm^{-3} sodium arsenate. Reproduced with permission from Ref. [51]. © 2012 Elsevier Ltd.

be ascribed to the formation of the products (MgO_2 ($Mg_3(PO_4)_2.2H_2O$, and MgF_2) complexes that prevented corrosive species in the electrolytes from reaching the metal alloy surface. Lamaka et al. [46] in their proof-of-concept work, tested the inhibitive performance of iron complexing agent on a commercial Mg in 0.5% NaCl solution. The complexing agent was found to substantially hindered the corrosive attack and suppressed evolution of hydrogen gas.

The degree of corrosion inhibition conferred by dissolved Li_2CO_3 on Mg alloy ZEK100 in 100 mM NaCl solution was evaluated, with a special focus on Li incorporation into the surface layer that forms under activated anodic dissolution (anodic polarization) [47]. When supplied at a concentration (100 mM) slightly below saturation, dissolved Li_2CO_3 lowered corrosion by a factor of 12. The transition to filament-like corrosion and concomitant anode/cathode activation, which begins at local breakdown sites, must be suppressed for effective suppression. The production of Li-doped MgO as a corrosion product film during activated anodic dissolution was linked to this inhibition. The chloride ion distribution with the film was strongly affected by the film composition when generated via anodic polarization. Chloride ions tend to enrich near the film/metal contact without Li insertion, whereas chloride ions tend to be equally distributed within the film with Li incorporation.

Inorganic substances that have been found to be effective in inhibiting the corrosion of Mg and Mg alloys are briefly highlighted below.

2.1.1. *Vanadate*

This is an anionic coordination complex of V. Most often, vanadate is used to describe the oxoanions of V and most of which exist in its highest oxidation state of +5. Feng et al. [44] investigated the effect of aqueous vanadate on the corrosion of AZ31 Mg alloy. The corrosion inhibition performance of aqueous vanadate was shown to be dependent on the pH of the solution. The most corrosion protection was provided by tetrahedral coordinate vanadate. The outcome of Feng et al. [44] is consistent with previous reports on Al [48,49]. The protection mechanism, on the other hand, is different. While vanadate's adsorbed polymerized film suppressed the oxygen reduction reaction on Al [48], it is less effective in suppressing the water reduction reaction on Mg. Corrosion protection on Mg appears to be due to anodic inhibition by adsorbed tetrahedral species.

2.1.2. *Arsenate*

As is a potent hydrogen evolution poison that prevents monoatomic hydrogen from combining on metal surfaces, resulting in a decrease in cathodic kinetics [50]. Arsenate is an oxidizing oxyanion of As, therefore it is likely that it will be reduced to generate As on Mg during corrosion. On pure Mg, Eaves et al. [51] investigated the performance and mechanism of an arsenate inhibitor in a 5% (w/v) aqueous NaCl solution. The extent of corrosion inhibition was determined by the amount of arsenate in the solution and the pH of the solution. When the concentration of arsenate was greater than 10^{-4} M, the rate of hydrogen evolution was significantly slowed. Figure 3 depicts the influence of pH on the corrosion inhibition. It is observed that at pH of 4 and below, the hydrogen evolution substantially repressed but increases with increase in pH. It was proposed that at pH 2–4, arsenate profoundly inhibited the Mg corrosion because it acted as a hydrogen atom recombination inhibitor through the electrodeposition of elemental As at active hydrogen evolution cathode sites [51]. At pH 6–8, arsenate only delayed but not prevented the onset of rapid Mg corrosion because it behaved as a precipitation inhibitor through the formation of insoluble $Mg_3(AsO_4)_2$ at active hydrogen evolution cathode sites. Eaves et al. [51] held that under acidic conditions (pH $\leq$ 4), precipitation of $Mg_3(AsO_4)_2$ was unlikely to take place because of the difficulty associated with the production of a local pH high enough to form AsO_4^{3-} even at local cathode sites.

2.1.3. *Chromate*

Chromate has proven to be more effective than a variety of other inhibitors [52]. It was found to outperformed various inhibitors including fluoride, phenyl phosphonate, silicate, oxalate, and carbonate, in pH and concentration-controlled circumstances when Mg was immersed in a 5% (w/v) NaCl solution for 1 h [52]. Schmutz et al. [53] investigated the effect of dichromate on the prevention of Mg corrosion in a 0.1 M NaCl solution. The addition of 10^{-4} M $Na_2Cr_2O_7$ considerably reduced the corrosion rate of uniform corrosion of Mg. However, filiform localized corrosion was observed. It was noticed that the uniform corrosion rate increased dramatically at the filiform localized corrosion locations. The concentration of $Na_2Cr_2O_7$ can be raised to prevent filiform corrosion. Filiform corrosion can still be triggered by scratching the surface coating, implying that the surface film is easily destabilized. Cr is a particularly good corrosion inhibitor on Mg in general. It can be used as a benchmark for other inhibitors.

2.1.4. *Phosphate*

Phosphate has a long history of usage as an inhibitor, particularly for steel corrosion prevention. Phosphate anions can

produce insoluble precipitates when they bond with a variety of metal cations. The production of insoluble $Mg_3(PO_4)_2$ is depicted as:

$$3Mg^{2+}{}_{(aq)} + 2PO_4{}^{3-}{}_{(aq)} \rightarrow Mg_3(PO_4)_2\downarrow \quad (7)$$

Williams et al. [52] compared the inhibition performance of phosphate, chromate, and other common inhibitors on pure Mg in a 5% (w/v) aqueous NaCl solution using the scanning vibrating electrode technique (SVET). Phosphate was found to perform outstandingly and its performance was linked to the concentration of the inhibitor and the pH of the solution. The protective efficiency rose as the phosphate content was increased from 10^{-4} to 10^{-2} M. The pH of the solution had a significant impact on inhibition. The inhibitory efficiency was lower when the pH of the solution was too high or too low. In neutral settings, $H_2PO_4^-$ and HPO_4^{2-} were the main aqueous species. At high pH, the phosphate ion, PO_4^{3-} takes precedence. Figure 4 depicts the phosphate protection mechanism at neutral pH. Localized corrosion on Mg occurred when it was exposed to a phosphate-containing NaCl solution, as shown in Fig. 4a. Due to hydrogen evolution, the pH of the localized sites rose, and HPO_4^{2-} deprotonated to generate PO_4^{3-} as the solution pH rises (Fig. 4b). The precipitation of insoluble $Mg_3(PO_4)_2$, which covered the surface and formed a protective film was triggered by a localized concentration of PO_4^{3-}. Because deprotonation of HPO_4^{2-} to PO_4^{3-} is limited at low pH (<4) and the solubility of $Mg_3(PO_4)_2$ is larger, inhibition was weak. Inhibition performance also diminished at very high pH (>10). At such pH, the concentration of PO_4^{3-} in solution is high and leads to homogenous precipitation of solution phase Mg^{2+} and PO_4^{3-} rather than surface film formation. $Mg_3(PO_4)_2$ is rapidly formed at pH 10 but not as a protective deposit on the alloy surface. Phosphate inhibition of Mg in near-neutral solutions is equivalent to chromate inhibition. In addition to being less poisonous than chromate, phosphorus offers another advantage. The precipitation-based protection mechanism works well in the pH range of 4–10.

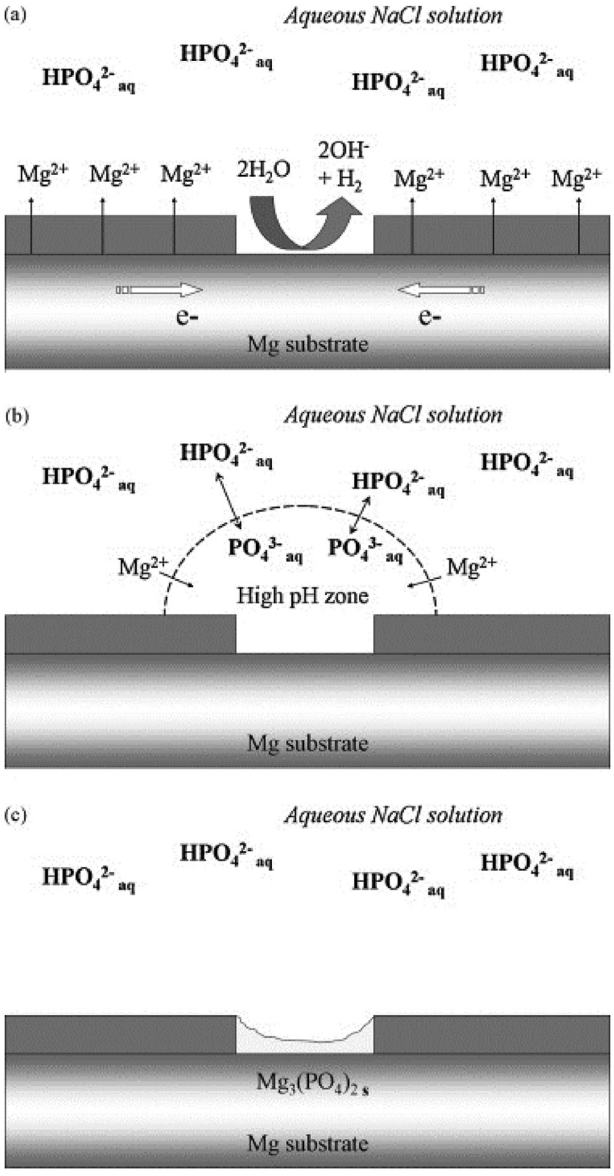

Fig. 4 – Schematic representation of the mechanism of Mg corrosion inhibition by aqueous phosphate ions at neutral pH, showing (a) localisation of the early stages of corrosion, (b) phosphate speciation in the vicinity of the local cathode and (c) deposition of an insoluble film. Reproduced with permission from Ref [52].

The inhibitive performance of inorganic compounds on the corrosion of Mg and its alloys are summarized in Table 1. Although some of these inorganic compounds are effective, the concern on their harmful effect due to their toxicity is forcing its reduction in industrial applications.

2.2. *Organic corrosion inhibitors*

Organic inhibitors inhibit corrosion by adsorption at the metal/solution interface. The heteroatoms like O, N and S as well as double and triple bonds in organic compounds serve as the interaction center. Some of the compounds studied as inhibitor for Mg and its alloys are discussed below.

2.2.1. *Surfactants*

Surfactants are surface-active substances that reduce interfacial tension or free energy at surfaces significantly. Surfactant molecules are amphiphilic, meaning they have both hydrophilic and hydrophobic sections [57], as well as a lengthy hydrocarbon tail and a tiny ionic or polar head group. Depending on the nature of their head groups, amphiphiles can be ionic (cationic, anionic), zwitterionic, or nonionic. Surfactants have been extensively investigated for their ability to inhibit corrosion. The corrosion inhibition efficacy of a wide range of surfactants is described in a considerable amount of scientific literature [58,59]. The concentration and amphiphilic qualities of the surfactant, as well as surface features such as charge, defects, and composition, all influence surfactant adsorption. Surfactants' hydrophilic hydrophobic nature causes interfacial adsorption and aggregation.

Sodium dodecylbenzenesulfonate (SDBS) is an anionic surfactant with excellent biological degradability that is commonly used in industrial and household detergents. For some metals and alloys, it has been identified as a type of ecologically friendly corrosion inhibitor. SDBS works as a

Table 1 – Summary of inorganic corrosion inhibitors for Mg and its alloys.

S/N	Inhibitor	Mg/Mg Alloy	Medium	Inhibitive pH	Conc. (mM)	IE%	Ref.
1	Vanadate	AZ31	0.1 M NaCl	9.2	–	–	[44]
2	Na_2CO_3	AZ31	0.1 M NaCl	–	50	76	[54]
3	Phosphate	WE43	0.5 M NaCl	Varies	–	–	[55]
4	KNO_3	Mg	0.5 wt.% NaCl	11	50	97	
5	KNO_2	Mg	0.5 wt.% NaCl	10.9	50	77	
6	KCN	Mg	0.5 wt.% NaCl	10.5	50	94	
7	NaSCN	Mg	0.5 wt.% NaCl	10.6	50	59	[27]
8	Na_3PO_4	Mg	0.5 wt.% NaCl	11.4	0.2	86	
9	NaF	Mg	0.5 wt.% NaCl	11.7	50	67	
10	$Ce(NO_2)_3$	Mg	0.5 wt.% NaCl	7.4	5	58	
11	Na_2MoO_4	WE43	0.05 M NaCl	–	50	94	[56]

mixed inhibitor for Mg alloys, inhibiting both the anodic and cathodic processes at the same time. The efficiency of inhibition improves as the concentration increases, while temperature has little effect on the efficiency of inhibition.

Frignani et al. [60] investigated a number of surfactants (sodium salt of N-lauroylsarcosine (NLS), N-lauroyl-N-methyltaurine (NLT), dodecylbenzensulphonic acid (DBS) or sodium lauryl sulphate (LS)) towards AZ31 Mg alloy corrosion in a 0.1 NaCl and 0.05 M Na_2SO_4 media. The inhibition efficiency values obtained from the investigation from the electrochemical impedance spectroscopy technique are given in Table 2. From the table, the best inhibition performance is noted for DBS whereas NLT exhibits the least. According to the authors [60], the inhibiting effects of the surfactants is due to a rapid adsorption on the alloy surface, which limited the cathodic reaction, followed by a precipitation stage with Mg^{2+} ions that made the inhibiting layer thicker and less defective, so that, over time, the anodic oxidation was almost blocked in a wide potential interval.

An anionic gemini surfactant based on an ethylenediaminetetraacetic acid, sodium 2,2′-(7,16-dihexyl-8,15-dioxo-7,10,13,16-tetraazadocosane-10,13-diyl)diacetate prepared by treating ethylenediaminetetraacetic acid dianhydride with N-dihexylamine had also been investigated as inhibitor for AZ31 alloy [61]. The surfactant functioned as a mixed type of inhibitor and inhibition efficiency depended on concentration and temperature increasing with increase in concentration but depreciating upon a rise in the temperature of the corrosive system. Changes on the surface of the alloy, such as desorption of the inhibitor, fast etching, and so on are usually responsible for depreciation in inhibitor's performance with increasing temperature.

Lu et al. [62] studied the corrosion inhibition performance of sodium dodecyl sulphate (SDS) on AZ91 Mg alloy. The study was done using hydrogen evolution and electrochemical techniques. The volume of H_2 of the specimen exposed to NaCl solution increased roughly linearly, whereas the H_2 evolution of the Mg specimen was significantly reduced when immersed in SDS-containing NaCl solution (Fig. 5a). A higher concentration of SDS in the solution resulted in a decrease in the volume of H_2, implying that the inhibitory effect is regulated by the inhibitor concentration. The studied SDS also behaved as a mixed type inhibitor with effect on both cathodic and anodic corrosion reactions (Fig. 5b). Figures 6 and 7 show the effect of adding SDS on the microstructure and morphology of the surface and the cross-sectional area of the Mg alloy.

It is observed that the dissolution of Mg substrate is significantly reduced in the presence of 0.05 M SDS (Fig. 6a and b), resulting in a minor amount of corrosion products being deposited on the surface after immersion in 3.5 wt.% NaCl for 48 h. A considerable amount of corrosion products covers the free alloy (Fig. 6a, c). This is supported by the corroded samples' cross-sectional morphology (Fig. 7). After a 48-h soaking, corrosion products accumulate on the Mg surface. When SDS was added, however, minimal corrosion products and a thin corrosion layer is found, indicating that the substrate is slightly damaged and covered by a protective corrosion layer. SDS has also been reported to inhibit the corrosion of AZ91 Mg alloy in 3.5 wt.% NaCl solution [63]. Generally, the mechanism

Table 2 – Percentage inhibition efficiency values from electrochemical impedance spectroscopy at 1, 24 and 168 h in 0.1 M NaCl and 0.05 M Na_2SO_4 in the presence of the various surfactants at 10^{-3} and 5×10^{-3} M concentration. Reproduced with permission from Frignani et al. [60]. © 2012 Elsevier Ltd.

Additive and concentration		After 1 h		After 24 h		After 168 h	
		0.1 M NaCl	0.05 M Na_2SO_4	0.1 M NaCl	0.05 M Na_2SO_4	0.1 M NaCl	0.05 M Na_2SO_4
1 mM	NLS	56	61	89	63	92	77
	NLT	35	6	82	37	78	56
	LS	62	33	78	51	88	76
	DBS	68	79	84	90	93	84
5 mM	NLS	58	14	83	68	84	73
	LS	6	0	79	62	84	68
	DBS	68	53	57	81	63	74

NLS, N-lauroylsarcosine; NLT, N-lauroyl-N-methyltaurine; DBS, dodecylbenzensulphonic acid; LS, sodium lauryl sulphate.

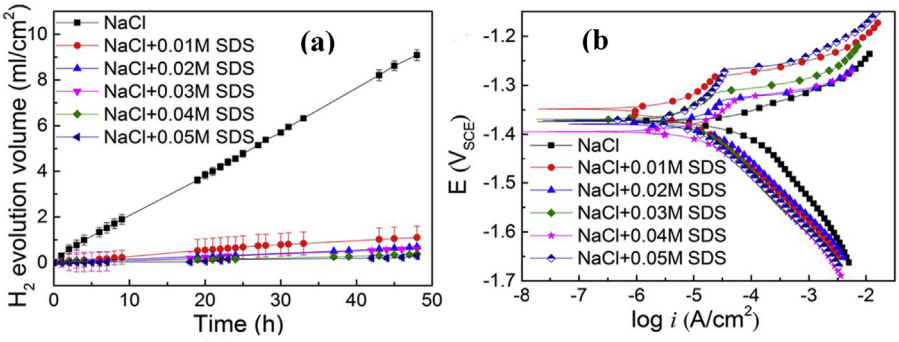

Fig. 5 – (a) Hydrogen evolution volume and (b) Polarization test of AZ91 Mg samples immersed in 3.5 wt.% NaCl with and without addition of different concentrations of SDS. Reproduced with permission from Ref. [62].

of inhibition by SDS is believed to involves the chemisorption of the surfactant molecules on AlMn intermetallics at the early stages of corrosion that decrease the cathodic reaction and micro-galvanic corrosion [62,63]. The inhibition of the anodic corrosion reaction has to do with the physisorption of high levels of SDS and the barrier effect of the surfactant occasioned by the long hydrophobic tail.

2.2.2. *Ionic liquids*

Ionic liquids (ILs) are a special type of substance made up solely of organic cations like alkylimidazolium, alkylpyridinium, alkylphosphonium, or alkylammonium and an organic or inorganic anion like tetrafluoroborate, hexafluorophosphate, tosylate, or bis(trifluoromethylsulfonyl) imide. They are soluble at room temperature and is due mostly to the cation's high degree of asymmetry that prevents crystallization at low temperatures. The anionic component is typically characterized by significant electron cloud delocalization and this also reduces interionic interaction. Furthermore, the huge number of potential cation and anion combinations have a wide range of polarity, hydrophobicity, and solvent miscibility properties.

In terms of "green chemistry," the use of ionic liquids has emerged as a new strategy due to their numerous intriguing

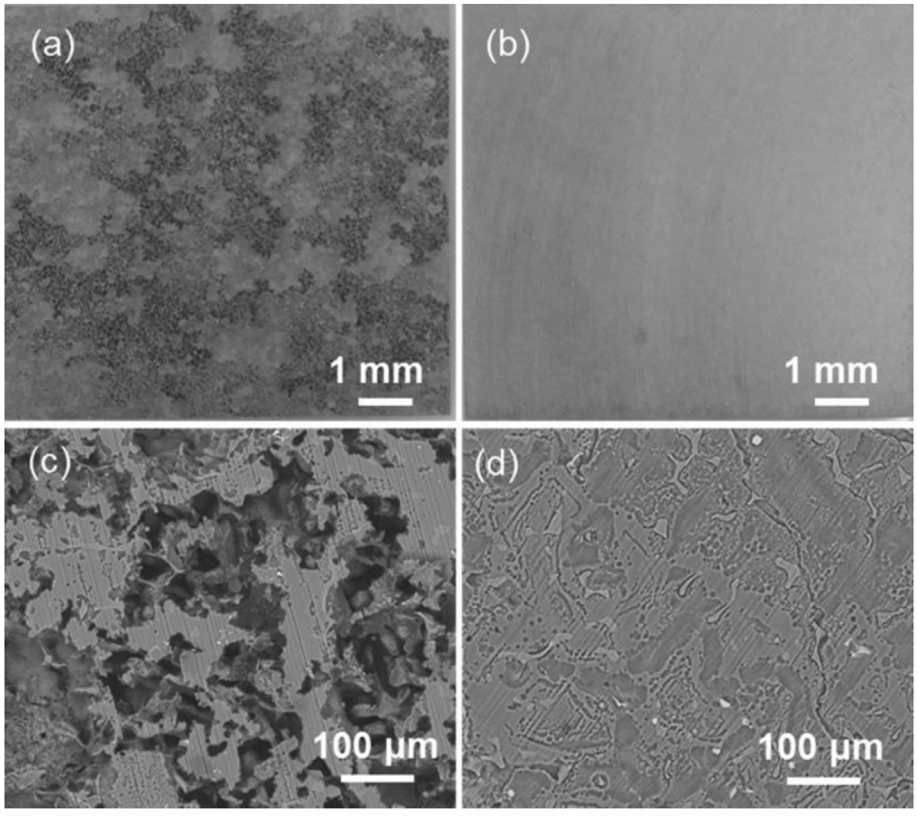

Fig. 6 – Surface morphology of Mg alloy after immersion for 48 h in blank NaCl solution (a and c) and NaCl with addition of 0.05 M SDS (b and d). Reproduced with permission from Ref. [62].

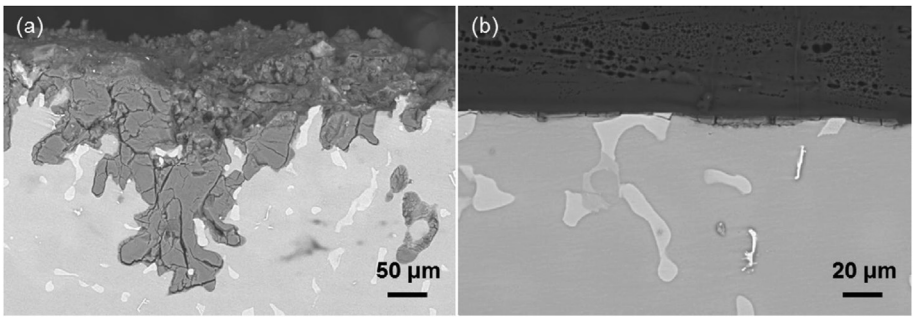

Fig. 7 – Cross-sectional morphology of Mg alloy after immersion for 48 h in blank NaCl solution (a) and NaCl with addition of 0.05 M SDS (b). Reproduced with permission from Ref. [62].

properties, including a lower melting point (below 100 °C), high polarity, low toxicity, lower vapor pressure, extremely high thermal and chemical stability, and a less hazardous impact on the environment and living beings. Other properties include high stability over a wide pH range, the ability to dissolve a wide range of organic and inorganic compounds, the ability to solubilize gases such as H_2, CO, and CO_2 and the dependence of solubility on the nature of cations and anions. The above-mentioned intriguing features qualified ionic liquids to be characterized as "green and sustainable chemicals" with the ability to dissolve a wide spectrum of inorganic and organic molecules, resulting in their widespread use in practically all sectors of chemistry and chemical engineering. Ionic liquids' appealing qualities also make them great candidates to replace traditional corrosion inhibitors, which have a number of negative consequences on the environment and living things. A great number of studies have been published in this area, detailing the use of ionic liquids as corrosion inhibitors [64–70].

Common types of ILs used for corrosion inhibition of Mg alloys are the imidazolium and long-chain phosphonium compounds but they are costly, unstable, and difficult to prepare. Other setbacks include short lifespan and adsorbed film peeling off easily, hence the need to design and synthesize cheap, efficient, and environmental friendliness ILs inhibitors. In this regards, Gao et al. [64] synthesized three novel ionic liquids, namely 1-n-butyl-2-hexylpyrazole bis(trifluoromethylsulfonyl) amide ([BHPz][NTf_2]), 1-n-butyl-2-octylpyrazole bis(trifluoromethylsulfonyl)amide ([BOPz][NTf_2]), and 1-n-butyl-2-decylpyrazole bis(trifluoromethylsulfonyl)amide ([BDePz][NTf_2]) (Scheme 1) and studied their corrosion inhibition ability for AZ91D Mg alloys in 0.05 wt.% NaCl solution. The ionic liquids performed satisfactorily with inhibition efficiency ranging from 75 to 90 °C (Fig. 8). It was observed that, the alkyl chain length has influence on the corrosion prevention property of the ionic liquids. At an inhibitor concentration of 20 ppm, the inhibition efficiency followed the sequence [BDePz][NTf_2] (90.0%) > [BOPz][NTf_2] (86.0%) > [BHPz][NTf_2] (83.1%) agreeing with the notion that long alkyl chain increases the inhibitive property of ILs by increasing the surface covering area [65]. However, many recent researches are attempting to answer the question of how long the alkyl chain length should be to induce maximum inhibition performance by ILs [65,66]. Ramachandran et al. [65] held that the chain length must be 12 or more carbon atoms.

Zheng et al. [67] reported the formation of protective film on AZ31B Mg alloy from the water soluble 1-butyl-3-methylimidazolium dibutylphosphate ([BMIM][DBP]) ionic liquid. Also, the challenges associated with ionic liquids as inhibitor for Mg and its alloys can be overcome through the use of surface functionalized nanoparticle tailored to function

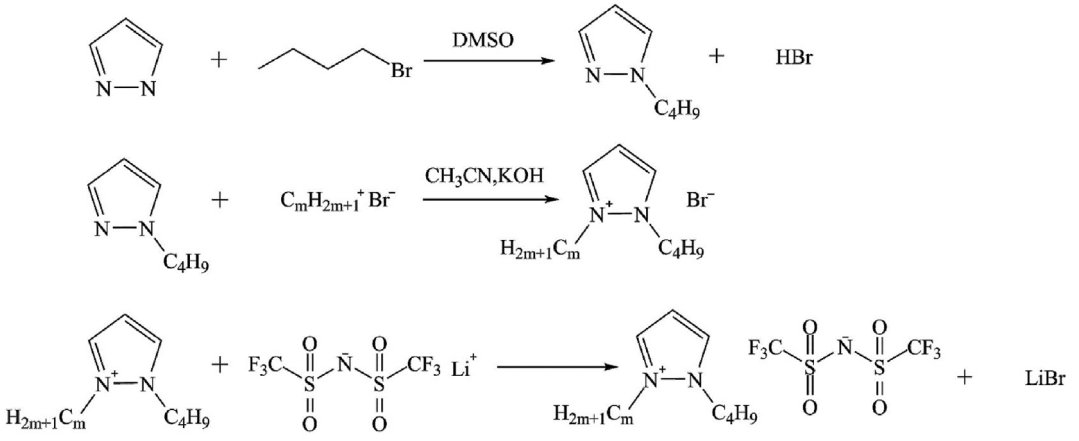

Scheme 1 – Synthetic route of [BHPz][NTf2] (m = 6), [BOPz][NTf2] (m = 8), and [BDePz][NTf2] (m = 10). Reproduced with permission from Ref [64].

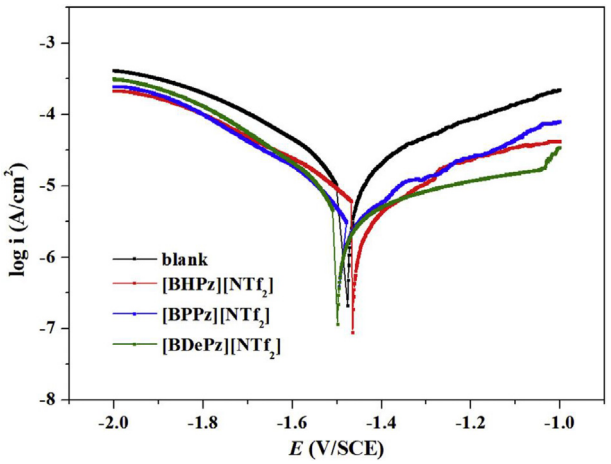

Fig. 8 – Polarization curves for AZ91D Mg alloy electrode in 0.05 wt.% NaCl without and with 20 ppm of different inhibitors. Reproduced with permission from Ref. [64].

as carriers of corrosion inhibitors, which can only be released intermittently based on demand, triggered by an altered pH, oxidation state and ion exchange [68].

The benzyl triphenyl phosphonium bis(trifluoromethyl sulfonyl)amide ([BPP][NTf_2]) was reported as a novel ionic liquid corrosion inhibitor for Mg alloy [69]. Using the Tafel linear polarization method, electrochemical impedance spectroscopy (EIS), and scanning electron microscopy (SEM), the inhibition of AZ31B Mg alloy in 0.05 wt.% NaCl solution was studied. At room temperature [BPP][NTf_2] had the highest inhibition efficiency of 91.4%. The adsorption of [BPP][NTf_2] on the surface of AZ31B Mg alloy followed the Langmuir isotherm, with chemical adsorption being the dominant mode. The FTIR analysis was used to detect the corrosive product. The effect of cation on inhibition, in addition to the influence of anion, was hypothesized as a possible inhibitory mechanism.

The corrosion inhibition behavior of the AZ31B Mg alloy by three imidazolium based ILs namely 1-ethyl-3-methy limidazolium bis(trifluoromethylsulfonyl)amide [EMIm][NTf2], 1-hexyl-3-methylimidazolium bis(trifluoromethylsulfonyl)amide [HMIm][NTf2], and 1-decyl-3-methylimidazolium bis(trifluoromethylsulfonyl)amide [DMIm][NTf2] was studied in 0.5 wt.% NaCl solution [70]. Electrochemical techniques complemented by surface analysis in combination with quantum-chemical computations were employed. The results obtained revealed that all the three ILs exhibited good corrosion inhibition efficiency. Among all the ILs investigated [DMIm][NTf_2] showed the best corrosion inhibition performance. The experimentally measured and theoretical computed results revealed that the inhibition efficiency of the ILs followed the order: [DMIm][NTf_2] > [HMIm][NTf_2] > [EMIm][NTf_2]. Furthermore, an increase in the inhibitor concentration led to an increase in the inhibition performance. The maximum inhibition efficiency of 93.91% with an inhibitor concentration of 1.0 mM for [DMIm][NTf_2] was obtained. Potentiodynamic polarization results indicated that all the investigated ILs acted as cathodic-type inhibitors.

2.2.3. *Schiff bases*

Schiff's bases are aldehyde or ketone compounds with an azomethine or imine group in place of the carbonyl group. They are frequently utilized in industry and demonstrate a wide spectrum of biological activity. They are also utilized as organic synthesis intermediates, catalysts, pigments and dyes, polymer stabilizers, and other applications. They have been widely reported as corrosion inhibitors for ferrous and non-ferrous metals [71]. Relative to other metallurgies, there are few reports on Schiff bases as corrosion inhibitors for Mg and its alloys. It had however been shown that Schiff bases have a high affinity to Mg^{2+} [72], inferring high possibility of complex formation between Schiff bases and Mg^{2+}. Ma et al. [73] synthesized three new Schiff bases from paeonol and amino acids (Fig. 9) and tested as corrosion inhibitors for Mg-Zn-Y-Nd alloy.

It was found that after seven days of immersion of Mg-Zn-Y-Nd alloy in 0.9 wt.% NaCl solution containing the different inhibitors at 37 °C, the corrosion resistance of Mg-Zn-Y-Nd alloy improved significantly with the maximum inhibition efficiency of 74%, 90%, and 91% for PCTyr, PCPhe, and PCCys, respectively at optimum concentration of 5×10^{-3}, 1×10^{-2}, 1×10^{-2} M. The alloy suffered a severe corrosion damage in the uninhibited 0.9 wt.% NaCl solution with serious localized corrosion pits (Fig. 10a and b). In the corrosive solution containing PCTyr, PCPhe and PCCys, the alloy surface was protected by a relatively flat, compact, and complete film formed on Mg surface (Fig. 10c–h). Ma et al. proposed that the Schiff bases inhibited the alloy's corrosion by reacting with Mg^{2+} ions to form complexes on Mg surface in the inhibitors-containing electrolytes. According to the authors, the phenolic hydroxyl groups in the molecular structure of Schiff bases (Fig. 10) were deprotonated after inhibitors containing solutions immersion as shown in Scheme 2 [73]. Thereafter, the inhibitor anions reacted with Mg^{2+} ions to form complexes that precipitated on Mg surface (Scheme 3) [73] and combined with corrosion products to form a more compact film on the metal surface which resulted in the reduction of the corrosion rate of Mg alloy.

Schiff base N′-bis (2-pyridylmethylidene)-1,2-diiminoethane (BPMDE) had also been investigated as inhibitor for AZ31 Mg alloy in 0.01 M HCl [74]. It was found that 20 mM BPMDE afforded inhibition efficiency of 62% after 24 h of immersion at 25 °C.

2.2.4. *Other organic compounds*

Benzotriazole is an effective corrosion inhibitor for Cu, Fe and Al alloys but acts in an unprecedented manner when use for Mg alloy [75–77]. It was found to show a slight inhibition of Mg corrosion in sodium chloride solution at a low concentration of 0.0005 M but the corrosion rate increased at higher concentration [27]. Ostanina et al. [77] reported that benzotriazole effectively inhibited Mg dissolution intensity under external anodic polarization at a concentration of 0.002 M. However, the effectiveness declined sharply with increase in concentration.

Long chain organic compounds like carboxylic and amides have been noted to exhibit high corrosion inhibitive effect for Mg alloys [23,78,79]. They act as a cathodic [78] and as a mixed kind of corrosion inhibitors [23,79,80]. Hu et al. [81] explored

PCTyr
Paeonol Condensation tyrosine

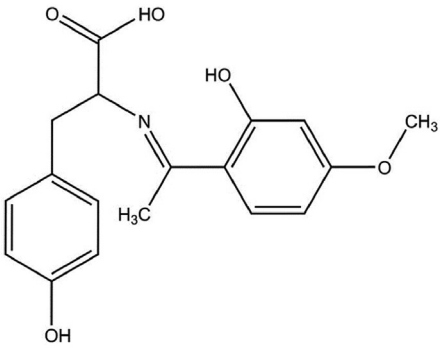

PCPhe
Paeonol Condensation phenylalanine

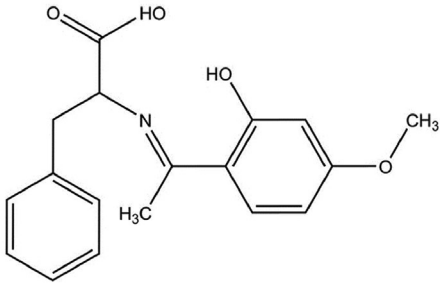

PCCys
Paeonol Condensation cysteine

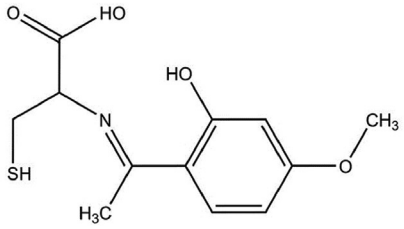

Fig. 9 – Chemical structures of the Schiff bases studied by Ma et al. [73].

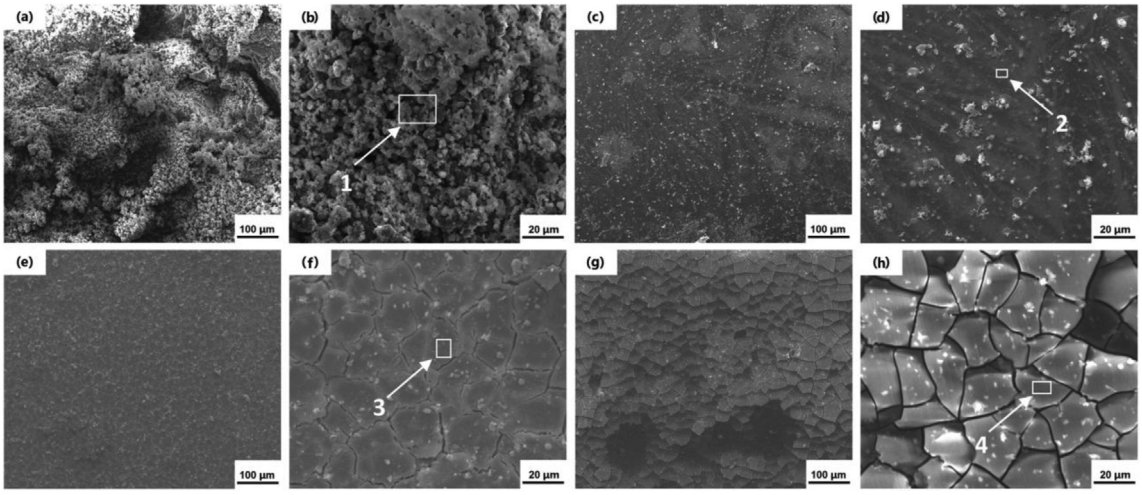

Fig. 10 – Corrosion morphologies of Mg-Zn-Y-Nd alloy after 7 days immersion in 0.9 wt.% NaCl solution: (a–b) without inhibitor (c–d) with 5×10^{-3} mol/L PCTyr (e–f) with 1×10^{-2} mol/L PCPhe and (g–h) with 1×10^{-2} mol/L PCCys. Reproduced from Ma et al. [73].

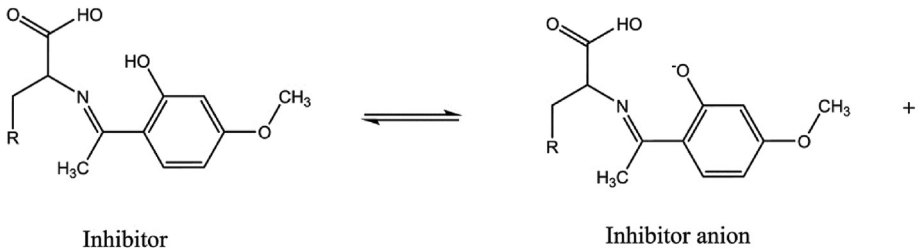

Scheme 2 – Deprotonation of Schiff bases [73].

the effectiveness of plant derived organic compound for Mg. They reportedly that isolated 2-hydroxy-4-methoxy-acetophenone from peony roots and skin, a known herb in Asian region, at 50 ppm concentration effectively inhibited AZ91D Mg alloy corrosion in 0.05 wt.% NaCl solution. The observed corrosion inhibiting effect was attributed to the formation of chelate complex between the organic compound with the Mg and reaction with $Mg(OH)_2$ to form a passive protective film which reduced the corrosion rate of the Mg alloy. Chirkunov and Zheludkevich investigated the effect of sodium dioctyl phosphate, 5-chloro-1,2,3-benzotriazole and 1,2,3-benzotriazole as inhibitor for the corrosion control of Elektron WE43 in 0.05 M NaCl solution using polarization and electrochemical impedance spectroscopy methods. Results obtained showed that sodium dioctyl phosphate exhibited high efficiency as inhibitor for WE34 Mg Alloy. Its inhibitive effect was due to the restrictive anodic partial electrode process and the effect increased with time as it forms slightly soluble complex with Mg that stabilizes hydroxide-oxide layer. However, both 1,2,3-benzotriazole and 5-chloro-1,2,3-benzotriazole under similar conditions was unable to inhibit corrosion of WE43 because the destruction of the protective barrier on the Mg alloy surface [26].

Dindodi and Shetty reported the corrosion inhibition of ZE41 Mg alloy in aqueous sulfate medium by stearate ($CH_3(-CH_2)_{16}COOH$). Stearate was found to be a mixed corrosion inhibitor but with dominant anodic influence. The inhibition efficiency increased with increase in concentration of the stearate until an aggregate transition concentration was reached, after which the efficiency decreased with further increase in concentration. Stearate inhibited the Mg alloy corrosion by virtue of adsorption which was noted to be physisorption [82]. Mai et al. [28] screened various compounds as corrosion inhibitor for Mg alloy in NaCl solution. The results are summarized in Table 3. The results reveal that most of the studied organic compounds accelerated the corrosion of the tested Mg alloys in NaCl medium solution at pH 6.8 ± 5. It was also found that smaller organic molecules did not appreciably affect the corrosion of CP mg and Mg-0.8Ca at low concentration in NaCl solution. Interestingly, uric acid and citric acid both independently inhibited CP Mg and Mg-0.8Ca from corroding in NaCl solution medium [28].

Sodium benzoate (SB) is the sodium salt of benzoic acid. SB has long been known to be safe as a direct food additive, as well as a corrosion inhibitor for steel, Zn, Cu and its alloys, Al and its alloys [83]. As a result, SB is a type of corrosion inhibitor that is friendly to the environment. The benzoic acid anion $C_6H_5COO^-$ is adsorbed onto the metal surface via carboxyl groups in a corrosion system including SB, lowering the free energy of the system and impeding the passage of metal ion–atoms from the lattice into the solution. The effect of SB on AM60 Mg alloy in 3.5% NaCl solution and influence of temperature on inhibition efficiency were investigated with electrochemical impedance spectroscopy (EIS), and polarization [84]. SB was discovered to be an effective inhibitor for Mg alloys exhibiting inhibition efficiency of more than 75% at 0.5 mol/L concentration. The adsorption of SB molecules on the alloy surface was found to follow physical adsorption mode. It was observed that the adsorbed SB molecules formed a multi-molecular layer on the Mg alloy surface to prevent the Mg alloy from contacting the corrosive solution. However, when SB concentration was up to 0.7 mol/L, the inhibition efficiency was found to be near constant and this was attributed to the dominance of intermolecular repulsion with increasing SB concentrations. Moreover, inhibition efficiency was also found to be near constant when temperature changed from 25 °C to 70 °C.

Lei et al. [85] investigated the inhibitory effect of hexamethylenetetramine (HMTA) on AZ31 Mg alloy in a simulated cooling fluid. Their findings revealed that HMTA had a strong inhibitory effect on the surface of the AZ31 Mg alloy. On AZ31, HMTA was found to be a mixed-type inhibitor, inhibiting both

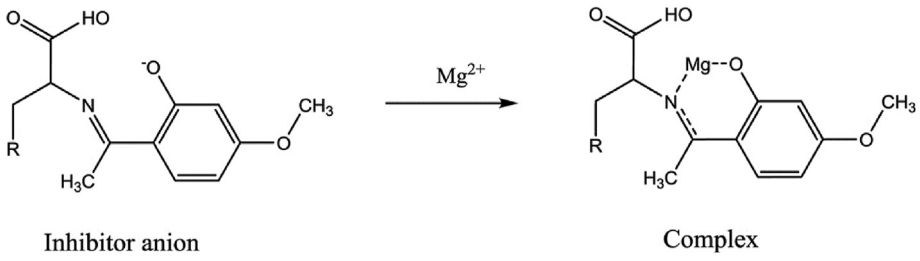

Scheme 3 – Complex formation between Schiff bases anions and Mg^{2+} [73].

Table 3 – Corrosion inhibition effect of some organic compounds for Mg alloy in NaCl solution. Reproduced with permission from Mai et al. [28]. © 2019 Elsevier Ltd.

Organic Compound	Concentration (M)	CP Mg Vol. H_2 (20 h)/mL	Mg-0.8Ca Vol.H_2 (20 h)/mL	CP Mg IE%	Mg-0.8Ca IE%	Remark	Ref.
Phenol red	2.82×10^{-5}	362.5	66.5	6	−6	CP-Mg inhibited	
B-Hydroxybutyric acid	9.00×10^{-6}	291.4	65.2	−1	−4	–	
Lactate	2.20×10^{-3}	395.1	62.6	−2	0	Mg0.8Ca inhibited	
Glucoronic acid	5.67×10^{-5}	360.9	66.9	7	−6	CP Mg Inhibited	[28]
Malic acid	6.70×10^{-5}	375.3	69.6	3	−11	CP-Mg inhibited	
Creatinine	1.00×10^{-4}	392.2	79.5	−2	−27	–	
Glycerol	1.87×10^{-4}	399.5	60.2	−3	4	Mg0.8Ca inhibited	
Urea	6.66×10^{-3}	340.1	67.7	12	−8	CP-Mg inhibited	
Uric acid	4.82×10^{-4}	294.8	51.9	24	17	Both	
Citric acid	1.66×10^{-4}	356.9	60.3	8	4	Both	
Succinic Acid	4.23×10^{-5}	397.2	68.4	−3	−9	–	
Acetone	3.44×10^{-4}	377.2	65.0	2	−3	CP-Mg inhibited	
Pyruvic acid	1.40×10^{-4}	426.5	72.7	−10	−16	–	

the anodic and cathodic processes. Slavcheva and Schmitt [86] reported the inhibitory effect of lactobionic-acid derivatives and 6-ring organic compounds containing N-heteroatom on Mg alloy AZ91 in 50 wt.% aqueous ethylene glycol (EG) solution. Lactobiono-tallow amide functioned as a mixed-type inhibitor, lowering the rates of both anodic and cathodic partial corrosion processes.

Amino acids are a unique family of biomolecules that include both amino (-NH_2) and carboxyl (-COOH) functional groups and are essential to all living things. They are important in processes such as neurotransmitter transport and biosynthesis, as well as serving as building blocks for proteins. They're used as a nutritional supplement and as a catalyst in the conversion of glucose to fructose in water. Amino acids are classified as α-, β-, γ-, and δ- and - amino acids, depending on where the amino functional group is connected. α -Amino acids, apart from glycine, have alkyl side chains, and the inductive action of the alkyl side chain has a significant impact on reactivity. Amino acids appear to meet the requirements of a green corrosion inhibitor in terms of non-toxicity, biodegradability, and non-bioaccumulation. Furthermore, they are water soluble and quite inexpensive. In recent years, there have been a significant rise in research into amino acids as a metal corrosion inhibitor [87,88].

Helal and Badawy [89] examined the corrosion inhibition of Mg-Al-Zn alloy in naturally aerated chloride-free stagnant neutral solutions utilizing amino acids as environmentally benign corrosion inhibitors. Pure amino acids were investigated, including aliphatic, aromatic, and sulphur-containing amino acids. Their findings revealed that the efficiency of inhibition was dependent on the chemical structure of the amino acid as well as its concentration. The amino acids containing aromatic rings and sulphur heteroatom in their structure exhibited better inhibiting effect.

Mg-10Gd-3Y-0.5Zr (GW103) is a rare-earth Mg alloy that can be used to make engine blocks. Many ethylene glycol (EG)-containing commercial coolants cannot provide sufficient corrosion protection for Mg alloy components in engine blocks. Hence, the use of effective corrosion inhibitors in engine coolants is necessary. Huang et al. [90] at 25 and 90 °C tested pyrazine and piperazine as corrosion inhibitors for the GW103 Mg alloy in EG solution. Pyrazine was found to be a better inhibitor than piperazine. From the weight loss technique and after 3 days of immersion, 500 ppm of pyrazine protected the GW103 Mg alloy in EG solution by 65.9% at 25 °C and 76.9% at 90 °C.

2.3. *Hybrid (inorganic-organic) corrosion inhibitors*

The synergistic effect of individual inhibitor molecules that are composed into hybrid manifest as an improved, effective control against the deterioration of Mg. The application of inorganic tetraethoxysilane (TEOS) in corrosion control is common due to its thermal stability and high stability in corrosive medium [91]. However, because Mg has a low melting point temperature, the resulting films on the metals surface are very susceptible to cracking, hence limiting the use of thick film layers and the high curing temperature of above 400 °C for the inorganic silane precursor alters the structure and mechanical properties of the Mg alloys. The current trend of synthesizing organic-inorganic inhibitors devoid of the challenges associated with TEOS is to modify silanes of the type (R—Si (OR)n-1) by substituting the R in the OR group with an organic (R) group. Zoubi et al. [92] used plasma electrolytic oxidation (PEO) and two step dip chemical coating (DCC) to formulate a hybrid of organic compound with an inorganic linker as a corrosion inhibitor for AZ31 Mg alloy. Chemical analysis of the hybrid showed that the presence of the linker facilitated the adsorption of the organic constituent of the hybrid onto the alloy. Further analysis via electrochemical study provided information on how the corrosion resistant of the Mg alloy was greatly improved due to the combined effect of the constituents in the hybrid. The combined effect of two heterocyclics has also been reported to enforce adsorption of organic-inorganic compound on corroding metal surface because of high electron donor sites [93].

Al Zoubi et al. [92,94] made a significant progress on the fabrication of hybrid materials on Mg alloys by using a functional binding agents (FBAs), $Mg(OH)_2$ or $Co(OH)_2$—$Mg(OH)_2$—$Co(OH)(NO_3)$ as an efficient tools for functionalizing surfaces, whereby the morphology and growth of the organic-inorganic material can be varied by altering the interfacial composition to achieve improved functionality. To

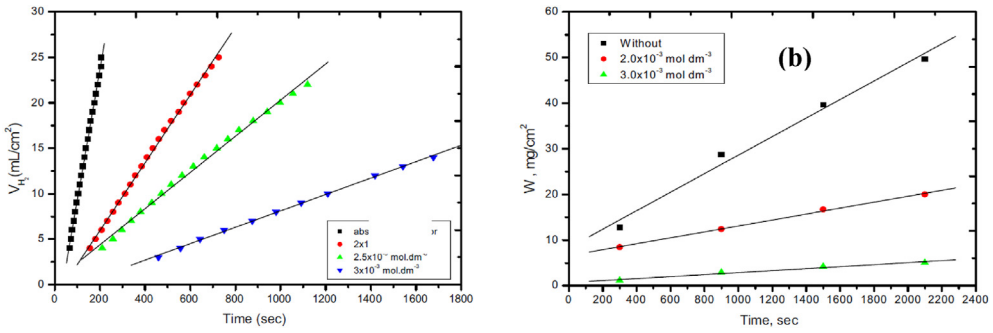

Fig. 11 – Plot of (a) hydrogen evolution vs time and (b) weight loss vs time in the absence and presence of inhibitor (PEG) for the corrosion of Mg in HCl acid [Reproduced from [101].

demonstrate the potential of this strategy, they combined PEO and DCC techniques to deliver multi-layered constructions of several chemical compositions consisting of inorganic and organic components. The single layer of FBAs was fabricated on the rough inorganic coating through chemical treatment using DCC, transforming it into a binding site for primary clusters of 2- mercaptobenzimidazole (MBI) molecules. As a result, the FBAs formed coordination complexes with organic molecules, which grew on FBA surfaces. Electrochemical studies revealed that the self-assembly of organic-inorganic hybrid heterostructures appreciably retarded the metal oxidation and oxygen reduction reactions, due to a synergistic effect arising from the combination of FBAs with organic and inorganic coatings.

Metal-organic framework composed of Al fumarate (AlFu) was synthesized for use as corrosion inhibitor for Mg alloy AM60B in 30% ethylene glycol with 0.5 M NaCl solution [95]. In a concentration range of 50–400 ppm, electrochemical impedance spectroscopy and potentiodynamic polarization techniques were utilized to assess the inhibitor performance. The results showed that the compound had a protection efficiency of about 88%. Potentiodynamic polarization measurements showed that the protection was primarily achieved by a reduction in the rate of the metal dissolution reaction. In a similar study, the corrosion of AM60B Mg alloy in ethylene glycol solution containing chloride ions was examined using Al terephthalate metal-organic framework (AlTp) and its nanocomposites [96]. Al terephthalate showed a high potential for usage as an inhibitor in ethylene glycol + water solution. It was found that adding a 10 wt.% nanoparticles such as graphene oxide or Fe_2O_3 to the inhibitor boosted inhibitory efficacy from 86.5% to over 90%.

Nashrah et al. [97] outlined the formation mechanism of hybrid organic-inorganic materials on light metals using PEO and DCC. The researchers pointed out that the interactions between organic molecules and the porous inorganic layer occurred through charge-transfer-type interactions and electrostatic interactions between the electron atom donor and the inorganic components in the coating surface. They showed that the superior corrosion protection effect by hybrid organic-inorganic materials is because of synergistic combination of individual components (i.e., organic and inorganic compounds) in enhancing structure compactness and chemical stabilities.

2.4. *Polymers as corrosion inhibitors*

Corrosion inhibition performance of polymers was reported by Umoren et al. [31] to be promising for Mg and its alloys. This class of compounds has been advocated for use in diverse areas. The advocacy for the utilization of polymers for corrosion control especially the natural polymers is due to the environmental friendliness property in accordance with the legislation passed by registration, evaluation authority and restriction of chemicals (REACH) with that of Paris commission (PARCOM) both emphasizing on green compliance of all chemicals [98]. The green compliance is in term of low toxicity, biodegradability, and non-bioaccumulation. All polymers of natural origin fall among the compounds that are certified by REACH and PARCOM for meeting their standards on chemical safety. In addition to the eco-friendly property, polymers are cheap, stable with multiple adsorption centers that enable them to meet the crucial requirement for a compound to be a corrosion inhibitor [99]. In the work of Umoren et al. [31], the effect of some of natural polymers such as dextran (Dex), alginate (ALG), hydroxyethyl cellulose (HEC), Gum Arabic (GA), pectin (PEC), chitosan (CHI) and carboxymethyl cellulose (CMC) on the corrosion inhibitive property of AZ31 Mg alloy in NaCl (3.5wt.%) solution was investigated. Only HEC and ALG of all the tested polymers were able to moderately inhibit the corrosion of the Mg alloy in the studied corrosive medium. HEC and ALG (1 g/L) inhibited the alloy corrosion by 64.13% and 58.27%, respectively.

Dang et al. explored the environmentally benign sodium alginate (SA) polymer as corrosion inhibitor for AZ31 Mg alloy in 3.5 wt.% NaCl solution [100]. SA molecular structure contains lipophilic alkyl groups and hydrophilic carboxyl groups making it easily adsorbed onto Mg surface and combined with $Mg(OH)_2$, thereby prompting effective protective composite film on the Mg surface that slowed down the rate of corrosion. Chain-entangling effect due to large molecular volume limits the corrosion inhibition efficacy of SA. In an attempt to overcome this problem, Hou et al. [100] explored the use of sodium phosphate (SP) to reinforce the corrosion inhibitive effect of SA. By using different combinations of the polymer and sodium phosphate such as 0.05 wt.% SA + 0.05 wt.% SP, 0.05 wt.% SA + 0.10 wt.% SP, 0.05 wt.% SA + 0.15wt.% SP and 0.05 wt.% SA + 0.20 wt.% SP, the corrosion inhibitive effect of the mixtures

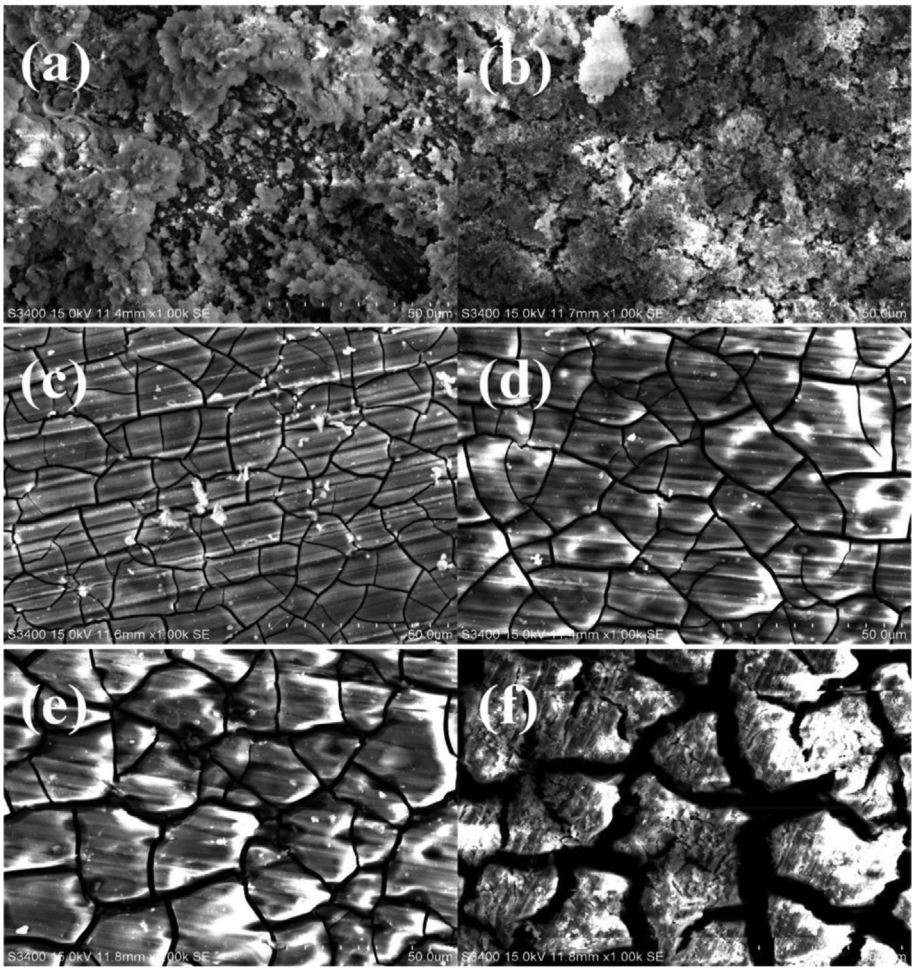

Fig. 12 – SEM images of WE43 Mg alloy after 3 days of immersion in 3.5 wt.% NaCl blank solution (a), and that with various PASP concentrations: (b) 400 ppm; (c) 600 ppm; (d) 800 ppm; (e) 1200 ppm and (f) 2000 ppm. Reproduced from [70].

for AZ31 Mg alloy at room temperature was found to increase tremendously reaching inhibition efficiency of 98%. Hassan et al. [101] used weight loss and gasometric techniques (Fig. 11) to investigate the effect of poly (ethylene glycol) (PEG) as an inhibitor for Mg corrosion in acidic (0.1 M HCl) medium. The effect of numerous parameters on corrosion rates, including inhibitor concentration and geometrical structure, corrosive medium concentration, and temperature was investigated. The efficiency of inhibition was observed to improve with raising the inhibitor concentration and, to a lesser extent, with increasing the temperature. A minute amount of PEG was found to show a profound inhibition effect in the corrosive environment. This was attributed to OH bridges formed between Mg metal and the substrate.

Polyaspartic acid (PASP) is one of the known effective inhibitors for Mg and its alloys. For example, Yang et al. [102] studied the performance of PASP as inhibitor for WE43 Mg alloy in a 3.5 wt.% NaCl solution. The inhibition efficiency was found to increase with increase in the PASP concentration reaching 94.2% at optimum concentration of 400 ppm. The SEM images given in Fig. 12 demonstrates the effectiveness of PASP as inhibitor for WE43 Mg alloy corrosion in NaCl solution.

The high corrosion inhibition performance of PASP for Mg can be associated with its ability to form PASP–Mg complex. When PASP is introduced into NaCl solution, the PASP anions penetrates the pores of $Mg(OH)_2$ surface film and chelate directly with Mg^{2+} ions. By so doing, PASP–Mg complex is formed and precipitated on the metal surface. The PASP–Mg complex precipitates effectively seal the film pores. The surface film thus consist of $Mg(OH)_2$ and PASP – Mg combined in a certain ratio which are responsible for the high corrosion protection ability of PASP.

2.5. *Plant extracts as corrosion inhibitors*

The ideal and easiest approach to reduce the adverse effect of organic molecules is substitution with less toxic alternatives. In this regard, there has been growing interest in the exploitation of biomaterials extract as corrosion inhibitors. In addition to their environmentally friendly and ecologically acceptable features, many plant extracts are low cost, readily available and renewable sources of materials of prospective industrial significance. These characteristics are justified by the abundant phytochemical constituents of the extracts, sharing many similarities with the molecular and electronic

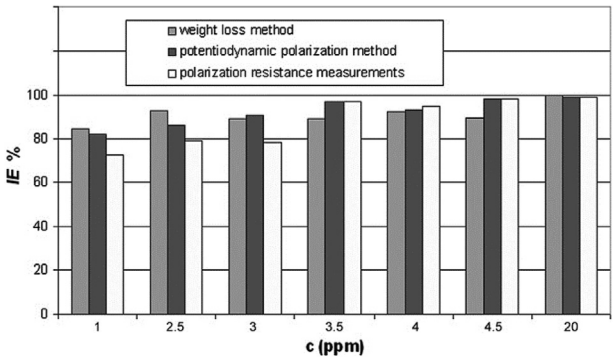

Fig. 13 – The comparison of inhibition efficiency data (IE%) for 3% NaCl solution with different concentrations of lavender oil obtained by weight loss method, potentiodynamic polarization method and polarization resistance measurements at 25 °C. Reproduced with permission from Ref. [107].

structures of conventional organic corrosion inhibitors, providing them the ability to adsorb onto metal surfaces. Extracts from their leaves, barks, seeds, fruits and roots comprise of mixtures of compounds containing heteroatoms often reported to function as effective inhibitors of metal corrosion in different aggressive environments [103–106]. A handful of research work has been carried out with plant extract as corrosion inhibitor for Mg and its alloys. Halambek et al. [107] studied natural oil extracted from *Lavandula angustifolia* leaves as corrosion inhibitor of Al-3 Mg alloy in 3% NaCl solution using weight loss, polarization measurements and SEM. The oil which was dissolved in ethanol and used was found to outstandingly inhibit the corrosion of Al-3 Mg alloy. The inhibition efficiency was found to reach 99% at 25 °C at inhibitor concentration of 20 ppm (Fig. 13).

Wu et al. [108,109] examined the performance of orange peel extracts (OPE) and extract of walnut green husk (WGHE) as inhibitor for AZ91D Mg alloy in 0.05 wt.% NaCl solution. OPE exhibited inhibition efficiency of 85.7% at 0.030 g/L while the optimal inhibition efficiency of WGHE was 44.8% at 1.0 g/L. However, by the immersion of the Mg alloys in 0.05 wt.% NaCl solution containing 1.0 g/L WGHE solution for 48 h, the inhibition efficiency increased to 92.5%.

2.6. *Synergistic inhibition effect*

Finding substances that can exert a synergistic effect when combined with an inhibitor, such that the quantity of an expensive inhibitor can be reduced or the efficiency of a moderately performed inhibitor can be enhanced, has been one of the steps taken by corrosion scientists to address the challenges of poor or moderate inhibiting ability of an inhibitor and that of exorbitant price in recent times. Synergism is a phenomenon in which the combined action of two or more compounds is larger than the sum of their separate actions. Synergism occurs in corrosion inhibitor systems either as a consequence of interaction between inhibitor formulation components or as a result of interaction between the inhibitor and one of the species present in the aqueous medium. Synergism can be considered an effective strategy for increasing inhibitor inhibitive force, reducing inhibitor usage, and diversifying inhibitor applications in corrosive conditions.

It is hypothesized that sodium phosphate and SDBS each operate as modest corrosion inhibitors on GW103 Mg alloy in an EG solution, but that the combination of sodium phosphate and SDBS as an inorganic-organic inhibitor package improves inhibition efficiency greatly [110]. According to Huang et al. [110], the inhibitive performance of phosphate-SDBS combination improved with increasing total inhibitor concentration but decreased with rising temperature. At low temperatures, the phosphate-SDBS combination was found to modify the GW103 Mg alloy surface film which led to a substantial synergistic inhibitory effect. Figure 14 shows the polarization curves of the GW103 alloy at various sodium phosphate: SDBS concentration ratios. The addition of the inhibitor has no substantial effect on the cathodic polarization curve. Anodic polarization current densities, on the other hand, are clearly diminished. The anodic inhibition is most likely to be due to the adsorption and deposition of the mixture on the GW103 surface, which inhibited the anodic dissolution more than the cathodic process. The polarization curves in Fig. 14 show that combining the organic and inorganic inhibitors in a specific ratio can provide much better corrosion protection than using individually.

Mg and its alloys have equally been inhibited by precipitation inhibitors such as tetraphenylporphyrin, organic sodium aminopropyltriethoxysilicate (APTS-Na), and inorganic zinc nitrate. These inhibitors could react with Mg^{2+} to generate insoluble compounds on Mg surfaces that slow down corrosion. 5,10,15,20-Tetraphenylporphyrin (TPP) was synthesized and its inhibition effect on AZ91D Mg alloy in 0.05 wt.% NaCl solution studied by Hu et al. [111]. Electrochemical measurement and immersion corrosion test results indicated that the inhibition efficiency of TPP reached 90%. It was found from surface analysis studies that TPP molecules chelated with Mg through their N atoms to form a TPP–Mg complex, which precipitated as a film on the AZ91D Mg alloy. The precipitated TPP–Mg reduced the porosity of the original $Mg(OH)_2$ surface film and retarded the dissolution of the Mg alloy. In ASTM D1384-87 corrosive water, both $Zn(NO_3)_2$ and APTS-Na exhibited a moderate corrosion inhibition impact on GW103 Mg alloy [112]. When these two inhibitors were combined, the inhibition efficiency reached over 95%. The strong synergistic effect between $Zn(NO_3)_2$ and APTS-Na on GW103 in the corrosive water was believed to arose from the deposition of $Mg(OH)_2$ and Zn(Mg) silicates that formed a compact protective film on GW103 [112].

3. Coatings containing corrosion inhibitors

The application of protective coatings to the surface of Mg metal has been the effective approach to ensure its durability. The “smart” self-healing notion is used in the most recent corrosion prevention technique in functional organic coatings. The storage of active species, such as corrosion inhibitors, in specialized carriers that are sensitive to certain stimuli, such as local pH changes, moisture uptake, mechanical rupture, or ion exchange, is a common feature of these coatings. These coatings can defend against active corrosion

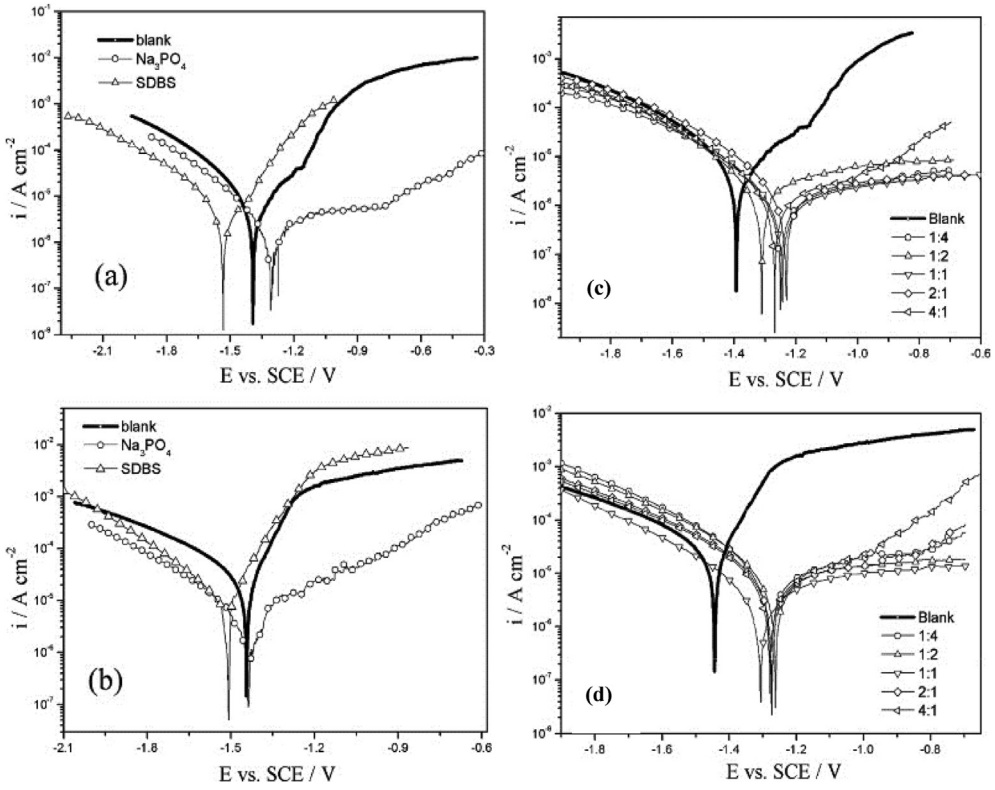

Fig. 14 – Polarization curves for GW103 in the 50% (vol.%) EG solution (a) at 25 °C, (b) 90 °C with and without 0.5 g/L Na_3PO_4 or 0.5 g/L SDBS; (c) 25 °C, and (d) 90 °C with various ratios of Na_3PO_4 over SDBS (the total inhibitor concentration 1 g/L). Reproduced with permission from Ref. [110].

by mending active corrosion locations and mitigating certain types of coatings damage, such as scratches or active corrosion sites. For instance, the protective effect of Si sol-gel coatings on Mg alloy AZ91 in 0.5 M Na_2SO_4 solution was improved by doping with Zr^{4+} or Ce^{3+} [113]. Therein, the Zr^{4+} and Ce^{3+} perform the function of inhibitor [114]. In another report, the inhibitive action of Zr sol-gel and Si sol-gel coatings on Mg alloy was enhanced via doping with 8-hydroxyquinoline inhibitor. The incorporation of the inhibitor prevented the deterioration of sol-gel matrix barrier properties in 0.005 M NaCl solution. Also, results on the corrosion behaviour of sol-gel coatings containing 2-methyl piperidine on AZ91D Mg in solutions containing 0.005, 0.05, and 0.5% NaCl showed that the corrosion resistance of the sol-gel coatings and sol-gel sealed phosphate conversion coatings were significantly improved through the addition of 2-methyl piperidine [115]. The inhibition effect of 2-methyl piperidine was more apparent at relatively low concentrations of NaCl or high concentrations of 2-methyl piperidine. Potentiodynamic polarization studies showed that 2-methyl piperidine, particularly at high concentrations, greatly reduced the anodic activity of AZ91D Mg alloy. Montemor and Ferreira [116] investigated the corrosion behaviour of AZ31 Mg alloy pretreated with a water soluble bis-aminosilane modified with multiwall carbon nanotubes (CNTs). Using the scanning vibrating electrode technique, the electrochemical behaviour of the silane-coated coupons was investigated while they were submerged in 0.05 M NaCl solutions. The electrochemical analysis revealed that the treated carbon nanotubes boosted the corrosion protection of the alloy. The analytical and microscopic investigation revealed that the CNTs were uniformly distributed throughout the silane coating and that they served as a platform for the storage of inhibitors.

On AZ91D Mg alloy, the corrosion-inhibition capacity of several corrosion inhibitors such as Ce^{3+}-Zr^{4+}, 8-hydroxyquinoline, and 2-mercaptobenzothaizole was investigated [117]. Inhibitors were placed into halloysite nanotubes (HNTs), which were subsequently end-stoppered with polymeric microcapsules and distributed in a hybrid silane matrix. Transmission electron microscopy was used to evaluate the surface morphology of raw and inhibitor-loaded HNTs, while Brunauer–Emmett–Teller and scanning electron microscopy/energy-dispersive X-ray spectroscopy were used to validate inhibitor encapsulation. Dip-coating was used to create the coatings on AZ91D coupons, which were subsequently thermally cured for 1 h at 130 °C. For varying lengths of exposure to sodium chloride solution of 0.6 M concentration, the anticorrosion effectiveness of inhibitor-encapsulated, HNT-based solgel coatings on AZ91D Mg alloy was tested using electrochemical impedance spectroscopy and potentiodynamic polarization. The anticorrosion performance of coatings was also tested using salt spray according to ASTM B117 for a 168-h exposure period. Ce^{3+}-Zr^{4+}-loaded HNT-based coatings were found to have higher anticorrosion capabilities under prolonged exposure to the corrosive conditions, 0.6 M sodium chloride solution.

The effect of intercalating a corrosion inhibitor, 8-hydroxyquinoline (8HQ), onto a Mg–Al based layered double

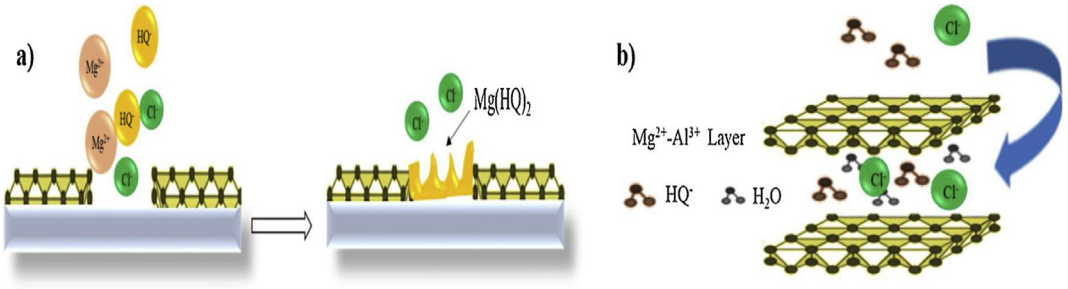

Fig. 15 – Schematics of corrosion inhibition mechanism of 8HQ intercalated Mg–Al LDH coating on AZ31. Reproduce with permission from Ref. [118].

hydroxide (LDH) coating on AZ31 was investigated [118]. In a 3.5% NaCl solution, the corrosion inhibition effect was tested using EIS and PDP techniques. It was found that 8HQ was successfully intercalated into Mg–Al LDH. The amount of 8HQ in the coating had a significant impact on its morphology. The ability to suppress corrosion was affected by both the structure and the concentration of 8HQ. For the optimum concentration (0.5 g) of 8HQ, corrosion resistance was significantly improved. The increase in 8HQ concentration over the optimal concentration had a detrimental impact on coating corrosion resistance. The following theories were proposed as the possible mechanism (Fig. 15) behind the improvement in corrosion resistance. (i)Because the LDH can exchange intercalated ions with solution, Cl^- was exchanged with intercalated 8HQ and entrapped in the LDH. Corrosion resistance improves as a result of this trapping. Furthermore, the intercalated 8HQ interacted with Mg^{2+} ions to create chelate. This chelates are deposited on the surface of LDH and may block active corrosive species [118], (ii) Chelates of 8HQ produced can self-heal, as previously documented [119]. It's possible that the $Mg(HQ)_2$ will precipitate and seal the defects. The increase in corrosion resistance of the coating is also due to the healing of defects. Furthermore, because of the lengthy exposure, the Cl^- reaches the substrate and pierces both the 8HQ layer and the outer layer. It's possible that it will react with Mg and release extra Mg^{2+} ions. These ions then react with HQ^- to form precipitates, which seal cracks and increase corrosion resistance once again [119]. The chemically adsorbed $Mg(HQ)_2$ also go through the dissolution process i.e. $Mg(HQ)_2 \leftrightarrow Mg^{2+} + 2HQ^-$ This dissolved HQ^- then chelates with Mg^{2+} ions and forms a surface deposit [118].

In 0.05 M NaCl solution, tri(bis(2-ethylhexyl)phosphate) (Ce $(DEHP)_3$) was utilized as a new corrosion inhibitor to protect AZ31 Mg alloy coated with an epoxy-silane hybrid coating [120]. $(DEHP)_3$ as a corrosion inhibitor, was made by combining three separate components in aqueous solution, including 2-(N-morpholino) ethanesulfonic acid monohydrate, $Ce(NO_3)_3.6H_2O$, and bis(2-ethylhexyl) phosphate salt, following the reaction scheme shown in Fig. 16.

Electrochemical impedance spectroscopy measurement revealed that the Ce $(DEHP)_3$-modified coating outperformed a reference coating in terms of corrosion resistance. The addition of a small amount of Ce $(DEHP)_3$ to the protective coating increased its barrier qualities, resulting in stable and long-term corrosion protection for the AZ31 Mg alloy. Furthermore, when the local pH reached alkaline levels, localized electrochemical experiments: (Localized electrochemical impedance spectroscopy (LEIS), scanning vibrating electrode technique (SVET), and scanning ion-selective electrode technique (SIET) revealed that Ce $(DEHP)_3$ was able to prevent corrosion progression at faults. The local inhibition of corrosion activity was correlated with the corresponding current density distributions and pH evolution using SVET and SIET measurements, confirming that Ce $(DEHP)_3$ retarded corrosion activity by acting as a pH-sensitive corrosion inhibitor. The combination of cerium and organophosphate resulted in the creation of stable/insoluble compounds that preserve the AZ31 Mg alloy from corrosion for a long time. Ce $(DEHP)_3$'s effective corrosion prevention action was confirmed in both intact and deteriorated coatings.

Na salt of 3-methylsalicylate (a derivatives of salicylic acid) was loaded into porous PEO coating Mg, which was additionally sealed by a polymer layer to prevent unintended loss of inhibitor in the electrolyte. Epoxy-silane based agents were applied as the primary components in the polymer for enhancing the barrier property and adhesion strength of the outmost layer. The hybrid PEO-epoxy coatings were tested for general corrosion for one month in a neutral (pH: 6.8–7.2) NaCl solution (3.5 wt.%) using the electrochemical impedance spectroscopy (EIS) method. Localized corrosion characterization technique, scanning vibrating electrode technique (SVET), was used to monitor the local current strength over scratched samples in 0.05 M NaCl solution for 24 h to

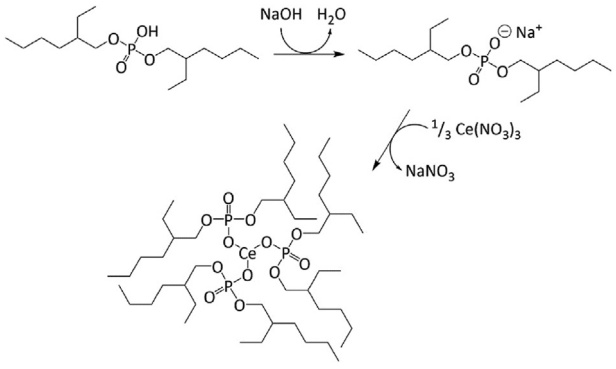

Fig. 16 – Reaction scheme for preparation of Ce $(DEHP)_3$. Reproduced with permission from Ref. [120].

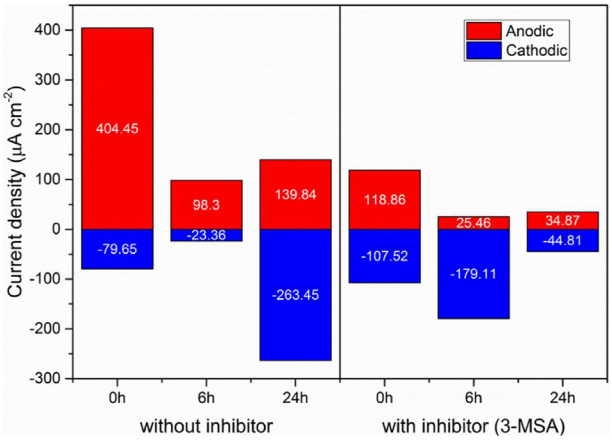

Fig. 17 – Peak current density (anodic and cathodic) on scratched PE-3S without and with inhibitor (3-methylsalicylate) during 24 h immersion in 0.05 M NaCl solution [Reproduced with permission from Ref. [121].

demonstrate the active corrosion protection capability caused by the inhibitor loaded in anodized layer [121]. The targeted characterization approach on artificially scratched specimens confirms the active protective performance imposed by the inserted inhibitors. As shown in Fig. 17, the electrochemically active regions (anodic and cathodic) and current density were lowered after a 6-h passivation interval by the integrated inhibitor. Physical/chemical adsorption and/or the creation of a complex between harmful impurity cations and inhibitor molecules have been proposed as two probable inhibitory mechanisms (Fig. 18).

Corrosion inhibitors are commonly used in coating systems as a cost-effective way to improve overall corrosion resistance and offer active corrosion protection qualities to coatings [122]. Indeed, the high porosity of the PEO layer has been investigated as a potential corrosion inhibitor reservoir. In most cases, an inhibitor is impregnated into a PEO coating by simply immersing the PEO-coated sample in a solution containing the inhibitor. Some organic and inorganic corrosion inhibitors have been added in PEO coatings on Mg alloys, with positive results in corrosion protection [123–126].

However, when the AZ21 substrate was coated with PEO, it was discovered that the presence of 2,5pyridindicarboxylate (2,5PDC) in the corrosive NaCl solution caused the coated sample to fail [127]. With an increase in 2,5PDC concentration in the electrolyte, both the beneficial inhibitory impact on bare AZ21 and the negative effect on the PEO layer were amplified. The key mechanisms of the 2,5PDC effect disparity were summarized as follows: (1) The Mg ions forms soluble complexes with 2,5PDC. The degradation of the PEO coating in the aqueous medium is accelerated by 2,5PDC due to the instability of $Mg_3(PO_4)_2$ and the promotion of MgO hydration. This leads to a faster obliteration of PEO's protective inner barrier layer, as well as the opening of routes for the corrosive medium containing Cl^- and O_2 to diffuse; (2) The inhibitory mechanism of 2,5PDC on Mg alloys involves the formation of a thick $Mg(OH)_2$/MgO layer, which inhibits Mg corrosion further. When compared to the already damaged inner barrier layer of PEO, the generated protective layer provides significantly weaker corrosion prevention properties. Furthermore, the additional mechanical stress imposed by the creation of this film on top of the PEO layer causes it to fail locally.

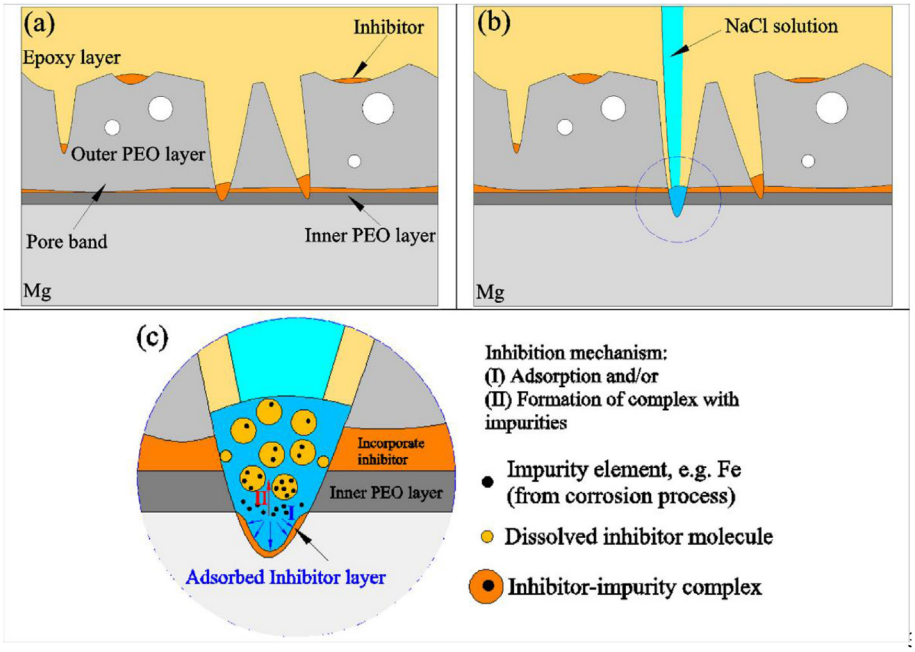

Fig. 18 – Schematic illustration of inhibition mechanism of inhibitor (sodium salt of 3 methylsalicylate). (a) Intact PE-3S-Inh coating (Cross-section morphology), (b) Occurrence of corrosion on the PE-3S-Inh coating and (c) Two plausible active protection mechanisms for incorporated inhibitor: (I) Physical/chemical adsorption and (II) Formation of Impurity–Inhibitor complex [Reproduced with permission from Ref [121].

Table 4 – Anti-corrosion properties of MgAl-LDHs coatings treated with various organic corrosion inhibitors.

LDH coatings	Substrate	Corrosive medium	Substrate i_{corr} ($\mu A/cm^2$)	LDH coatings i_{corr} ($\mu A/cm^2$)	Reference
LDH – PGA	AZ31	Hank's balanced salt solution	2.39	0.0895	[130]
LDH – PA	AZ31	0.1 M NaCl	59.40	0.76	[131]
LDH – MET	AZD91	3.5 wt.% NaCl solution	3.05	0.113	[132]
LDH – PPA	AZ31B	3.5 wt.% NaCl solution	14.90	0.00247	[133]
LDH – MSB	AZ31	3.5 wt.% NaCl solution	11.30	4.43	[134]
LDH – MKH	AZ31	3.5 wt.% NaCl solution	11.30	0.18	[134]
LDH – 8HQ	AZ31	3.5 wt.% NaCl solution	11.30	0.02	[134]

Note: the anion of LDH: PGA, poly-L-glutamic acid; PA, phytic acid; MET, methionine; PPA, phenylphosphonic acid; MSB, benzoic acid; MKH, 3-aminopropyltriethoxysilane; 8HQ, 8-hydroxyquinoline.

Various corrosion inhibitors have been introduced into LDH coatings in recent years to improve their inhibition or protection capacity [128–134]. Aspartic acid (ASP), an environmentally acceptable corrosion inhibitor, was intercalated into MgAl-layered double hydroxides (MgAl-LDHs) on AZ31 Mg alloy using a simple hydrothermal technique, and the MgAl-ASP-LDH coatings demonstrated excellent anti-corrosion and self-healing properties [128]. By combining co-precipitation and hydrothermal techniques, nitrate, molybdate and sodium dodecyl sulfate (SDS) were in-situ fabricated on AZ31 Mg alloy. The prepared LDHs films were dense and uniform, and closely combined with the substrate. The results obtained showed that the prepared three LDHs films dramatically enhance the corrosion resistance of AZ31 Mg alloy. The corrosion resistance of the LDHs films followed the order: MgAl–MoO_4^{2-} – LDHs < MgAl–NO_3^-–LDHs < MgAl-SDS-LDHs. The SDS intercalated LDHs film exhibited the best corrosion protection performance, due to the denser structure of the film and the inhibition of the adsorption of SDS anions on cathodic hydrogen evolution and anodic dissolution. In summary, the MgAl-LDHs films intercalated with SDS have great potential for improving the corrosion resistance of Mg alloys [129]. Table 4 summarizes the anti-corrosion properties of MgAl-LDHs coatings treated with various organic corrosion inhibitors.

There are some reports on the fabrication of MgAl-LDHs coatings modified with ionic liquids and their corrosion protection on Mg alloys. For instance, Jiang et al. [4] successfully fabricated two kinds of MgAl-LDHs coatings modified with imidazolium based dicationic ionic liquids, namely LDH-C_6 $(m_2im)_2$-I and IL@LDH- C_6 $(m_2im)_2$-PF_6 on AZ31B Mg alloy and evaluated their anti-corrosion properties in 3.5 wt.% NaCl solution. The structure of C_6 $(m_2im)_2$-I and C_6 $(m_2im)_2$-PF_6 is shown in Fig. 19. The LDH-C_6 $(m_2im)_2$-I coatings intercalated with C_6 $(m_2im)_2$-I ionic liquid was synthesized by the co-precipitation method and hydrothermal treatment, followed

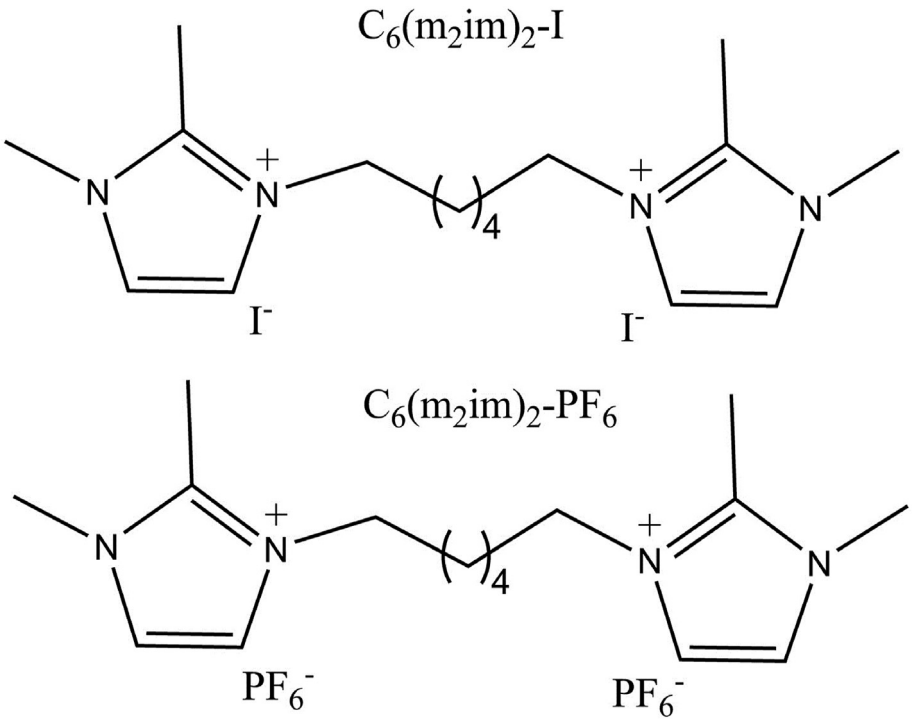

Fig. 19 – Structures of the two imidazolium based dicationic ILs. Reproduced with permission from Jiang et al. [4]. © 2022 Elsevier B.V.

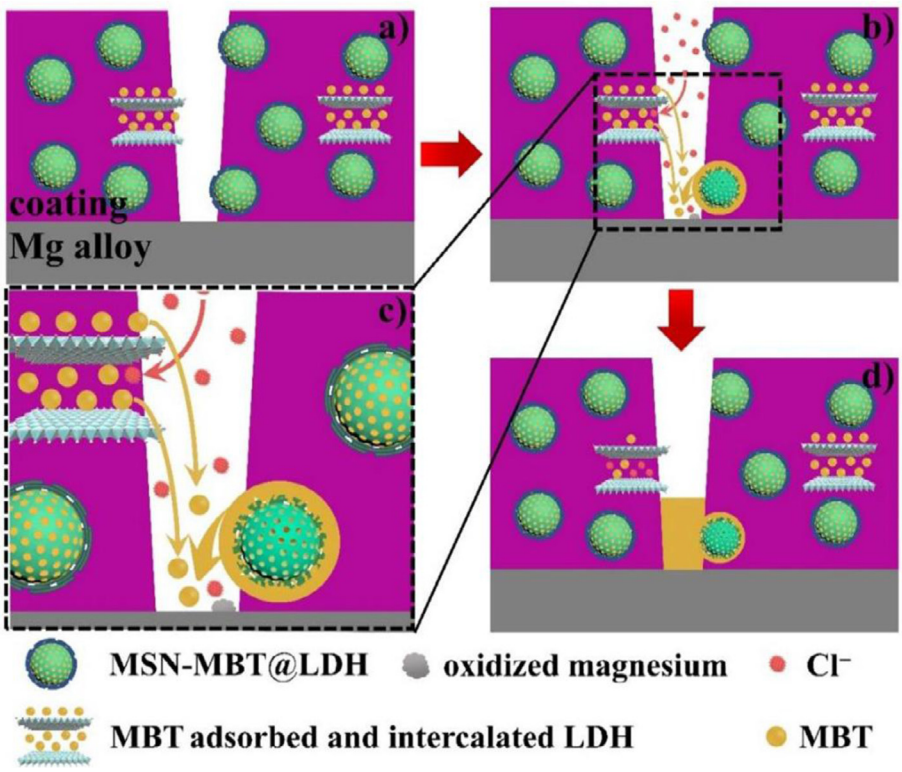

Fig. 20 – Schematic diagram for representation of the corrosion protection mechanism of the MSN-MBT@LDH nanocontainers incorporated SNAP coating on Mg alloy. (a) Nanocontainers incorporated hybrid coating with local damage (b, c) healing process including desorption of physically adsorbed MBT, release of intercalated MBT by ion exchange, and leakage of MBT from MSNs surface by the dissolution of LDH nanoshells, and (d) SNAP coating after self-healing [Reproduced with permission from Ref. [3].

by a facile immersion experiment in a DMSO solution containing C_6 $(m_2im)_2$-PF_6 ionic liquid to produce the IL@LDH-C_6 $(m_2im)_2$-I composite coating. It was found that the LDH-C_6 $(m2im)_2$-I coating exhibits a petal-like nanoflowers structure, while the IL@LDH-C_6 $(m_2im)_2$-I coating contains a compact C_6 $(m_2im)_2$-PF_6 IL film and a lamellar-structured LDH-C_6 $(m_2im)_2$-I, which provides a double corrosion protection to the AZ31B Mg alloy. The corrosion current density of IL@LDH-C_6 $(m_2im)_2$-I was estimated to be about thirty-eighth of that of LDH-C_6 $(m_2im)_2$-I and 4 orders of magnitude lower than that of bare Mg alloy, suggesting that the corrosion resistance of the IL@LDH-C_6 $(m_2im)_2$-I coating is obviously superior to that of the LDH-C_6 $(m_2im)_2$-I coating. More importantly, the surface of Mg alloy samples coated with IL@LDH-C6 (m2im)2-I remains compact without being destroyed after 168 h of immersion in 3.5 wt.% NaCl solution, exhibiting excellent corrosion protection performance on AZ31B Mg alloy. The anti-corrosion mechanism of the LDH-C_6 $(m_2im)_2$-I coatings was proposed as follows: (i) the LDH- C_6 $(m_2im)_2$-I film with highly compact petal-like nanoflowers structure serves as a protective layer to prevent the immediate contact between corrosive chloride anions and Mg alloy substrate, retarding the occurrence of the corrosion; (ii) because of the excellent anion-exchange ability of LDHs, the C_6 $(m_2im)_2$-I species in LDHs interlayers can be released to corrosive environments by exchanging with the corrosive chloride anions, which implies that the detrimental chlorides are ensnared into the interlayers and their concentrations will decline; (iii) the released C_6 $(m_2im)_2$-I species in corrosive environments are covered on the surface of LDHs by forming a corrosion inhibitor protective film, which provides a continuous corrosion protection to the Mg alloy.

Ouyang et al. [3] demonstrated the fabrication of pH-responsive nanocontainers consisting of corrosion inhibitor (2-mercaptobenzothiazole, MBT) loaded mesoporous silica nanoparticle (MSN) core and layered double hydroxide (LDH) nanosheet shell serving as gatekeepers. The mechanized MSN- MBT@LDH nanocontainers were obtained via a simple two-step adsorption process and show a pH-dependent release of MBT from MSN under acidic conditions. A smart corrosion protection system on AZ31 Mg alloy was obtained by incorporating the synthesized nanocontainers into a self-assembled nanophase particle (SNAP) coating. The electrochemical tests and visual observations show that the hybrid coating had the best barrier properties and robustness in corrosion protection in NaCl corrosive solutions in comparison with the control coatings. This was attributed mainly to the corrosion inhibition of MBT to the defects occurring at the coating-substrate interface and partially to the entrapment of aggressive Cl^- ions taking advantage of the excess LDH nanoplates that were not adsorbed on the MSN surface. The corrosion protection mechanism was summarized as follows: a certain amount of MBT is firstly released by dissolution of the LDH nanoshells of the nanocon-tainers owing to the

decreased pH value (~5.6) arising from dissolution of CO_2 from atmosphere in the water and formation of carbonic acid. The MBT molecules released from MSN-MBT@LDH nanocontainers can be adsorbed and deposited immediately at the defects of the Mg alloy by strong covalent Mg–S group to form a stable film to slow down both anodic and cathodic reactions [3], ensuring the pH values in the defect are close to neutral rather than quick alkalization of the solution to relatively high pH values. Mg and Al will be dissolved if the concentration of released MBT is not high enough to effectively suppress the corrosion processes. With the hydrolysis of dissolved Mg and Al cations, especially for the latter, the pH value in the anodic zones decreases further, possibly down to 4.8 [3]. The decreased pH accelerates the dissolution of LDH nanoshells and facilitates release of more MBT molecules, thus provides excellent and long-term corrosion protection properties to substrate in NaCl environments (Fig. 20).

The natural corrosive environment of physiological human fluid can cause substantial corrosion and mechanical damage to light Mg–Al alloys used in biomedical prosthesis. Rodrguez-Alonso et al. [2] investigated the effectiveness of hybrid sol-gel coatings with and without corrosion inhibitors, such as L-cysteine, TiO_2 nanoparticles, 2-aminopyridine, quinine, dimetyl glyoxime, and graphene oxide sheet, for the protection of AZ61 Mg alloy in Hanks' Balance Salt solution for 14 days immersion. The results demonstrated that adding an inhibitor to the sol-gel coating can increase corrosion performance greatly, and that it is an effective barrier for L-cysteine-doped hybrid sol-gel films. Other compounds, such as dimethyl glyoxime, quinine, 2-aminopyridine, or TiO_2 NPs, reduced the rate of corrosion of the sol-gel coating when introduced as corrosion inhibitors, but they degraded with time. In the chosen synthesis circumstances, sol-gel coatings doped with NPs such as graphene sheets did not perform well enough as corrosion inhibitors, but they appeared to enhance the formation of calciumphosphates (perhaps hydroxyapatite), thereby enhancing alloy biocompatibility.

Li et al. [135] described *in-situ* insertion of layered double hydroxides (LDH) nanocontainers into plasma electrolytic oxidation (PEO) coatings on AZ91 Mg alloy. Mg corrosion inhibitor fumarate was chosen for exchange and intercalation into the nanocontainers, which were then integrated into the coating. In the presence of LDH nanocontainers, the thickness and compactness of the coatings were observed to increase. The polarization test and electrochemical impedance spectroscopy were used to evaluate the corrosion protection efficacy of the blank PEO, LDH containing PEO, and inhibitor loaded coatings. Figure 21 shows the polarization curves of the coatings recorded in a 0.5 wt.% NaCl solution. The corrosion current density of PEO coating was lowered from 59.51 to 30.33 (PEO- LDH) and 14.81 μA/cm^2 (PEO-LDH-FA) according to the polarization curves, showing that the corrosion resistance of the layer was improved following the addition of LDH nanocontainer. After the corrosion inhibitor and nanocontainer were added, the coating's corrosion potential increases to −1.51 V. Furthermore, according to the anodic polarization curve, anodic dissolution is greatly delayed, which might be attributed to the influence of inhibitors in the coating. When corrosion occurs, the loaded inhibitor and nanocontainers were found to have a significant impact on the degradation process and corrosion resistance of the PEO coating, resulting in increased and stable corrosion resistance of the substrate.

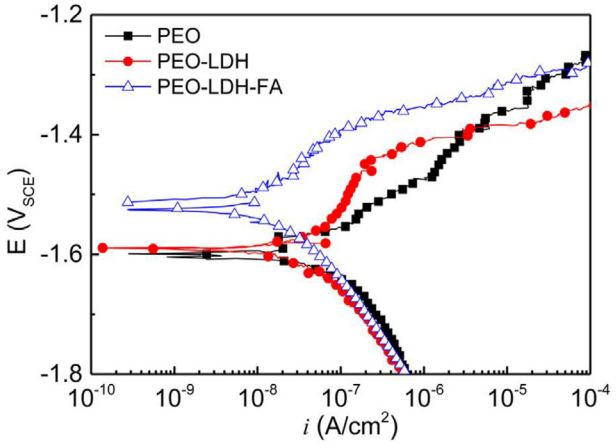

Fig. 21 – Potentiodynamic polarization of the PEO coatings in 0.5 wt.% NaCl [Reproduced with permission from Ref. [135]].

Some other reports on coatings containing corrosion inhibitors for the corrosion protection of Mg and Mg alloys in diverse corrosive media are summarized in Table 5.

4. Research gaps and future perspectives

1. Research on the use of corrosion inhibitors directly in corrosive solution to protect Mg and its alloys is limited. The reason might be due to the fact most compounds that perform effectively as corrosion inhibitors for other metals do not work for Mg and its alloys. For example, Chirkunov and Zheludkevich [26] found that azoles failed to inhibit the corrosion of WE43 alloy in 0.05 M NaCl solution. Lamaka et al. [27] screened 151 compounds (organic and inorganic) for anticorrosion property toward six alloys (AZ31, AZ91, AM50, WE43, ZE41 and Elektron 21) and three grades of pure Mg and noted that only 15 possessed anticorrosion property. Of the 15, 60% were compounds with high toxicity. Mei et al. [28] also noted that, 80% of 53 organic bio-compounds (amino acids, antibiotics, vitamins, and saccharides) investigated as corrosion inhibitors for CP Mg and Mg-0.8Ca alloys in chloride containing environment accelerated or minimally inhibited the corrosion of the alloys. We equally reported that chitosan, dextran, carboxymethyl cellulose, pectin, and Gum Arabic accelerated the corrosion of AZ31 Mg alloy in 3.5 wt.% NaCl solution [31]. Because there is a pressing need to inhibit the corrosion of Mg and its alloys due to the increasing industrial interest, future researches should be devoted to identifying low-cost, widely available, non-toxic, and environmentally benign compounds that possess high inhibitory effect for Mg and its alloys.
2. Information on the natural polymers and plant extracts as corrosion inhibitors for Mg and its alloys is very scanty. In the few reports on natural polymers as corrosion inhibitor

Table 5 – Anti-corrosion properties of coatings containing corrosion inhibitors for Mg and Mg alloys in diverse corrosive media.

S/N	Coatings systems with inhibitors	Substrate	Corrosive medium	I_{corr} of bare substrate ($\mu A/cm^2$)	I_{corr} of coatings systems ($\mu A/cm^2$)	I_{corr} coatings systems with inhibitor	Remarks/Findings	Reference
1	Mg/Al Hydrotalcites -2-mercaptobenzimidazole (2-MBT) inhibitor	AS21	Hank's solution	5.0×10^{-4}	2×10^{-5}	8.12×10^{-10}	The coatings containing 2-MBT as inhibitor gave lower current density in comparison with the bare coatings. A maximum efficiency of 92% was reached after 0.5 h and 75% in a period of 102 h	[136]
2	Shape memory polymers (SMP) based Superamphiphobic coatings - 1, 2, 3-benzotriazole (BTA) inhibitor	AZ31B	3.5 wt.% NaCl	1.90×10^{-4}	1.13×10^{-11}	2.88×10^{-12}	The Mg alloy with the coatings can withstand immersion in 3.5 wt.% NaCl solution for 80 days and neutral salt spray with 5 wt.% NaCl for 54 days. Furthermore, the coatings show excellent self-healing capability towards various physical damages, such as 10 scratching/self-healing cycles at the same position, hexagonal star scratching and grid scratching.	[137]
3	LDH – methionine epoxy coatings	Mg alloy	0.35 wt.% NaCl	9.981	–	6.736 @ pH 5 5.806 @ pH 7 1.687 @bpH 9	The Mg alloy@Met-LDHs at different pH (pH 5, 7 and 9) have a higher E_{corr} and a lower I_{corr}. Their passivation region may be due to the adsorption of methionine released from the Mg/Al LDHs interlayer to form a protective film. The Mg alloy@Met-LDHs under alkaline conditions (pH 9) has the lowest I_{corr} and corrosion rate, and a highest corrosion inhibition efficiency (83.09%).	[138]
4	Micro arc oxidation (MAO) – N 16 ([N-(5-hydroxypent-3-yl)-N,N-dimethylhexadecan-1-aminium bromide] inhibitor	AZ31	3.5 wt.% NaCl	1.936	4.612×10^{-2}	2.340×10^{-2}	The potentiodynamic polarization and electrochemical impedance spectroscopy measurements showed that compared with the MAO membrane covered Mg alloys, the organic-inorganic composite coating has superior corrosion resistance with a lower corrosion current and a higher protection efficiency (99.7%) after immersion in 3.5 wt.% NaCl solution, attributing to the synergistic effect of effective inhibition of inhibitor and the physical barrier ability of hydrophobic film and MAO membrane.	[139]
5		AZ31	3.5 wt.% NaCl	29	15			[140]

	Cerium conversion coatings with Mn $(NO_3)_2.4H_2O$ and polyvinyl alcohol (PVA) inhibitors					7 (Ce—Mn) 10 (Ce-PVA) 8.5 (Ce— Mn-PVA)	Addition of Mn and PVA to the Ce solution led to more uniform, denser and crack free coating deposition on the Mg AZ31 alloy surface. Inclusion of Mn^{2+} and PVA into the Ce solution resulted in inhibition of both anodic and cathodic reactions, with dominant effect on the cathodic reactions restriction. The Mg AZ31 alloy surface treatment by Ce coating in the presence of both PVA and Mn^{2+} cations resulted in meaningful improvement of the coating corrosion protection performance through increasing the coating barrier properties and reducing the number of galvanic couples existed on the Mg AZ31 alloy surface.	
6	Silica based sol-gel coatings containing quinaldic acid (QDA), betaine (BET), dopamine hydrochloride (DOP), and diazolidinyl urea (DZU) inhibitors.	AZ31B	3.5 wt.% NaCl	—	—	—	Coatings were defect-free and provided enhanced protection, as observed from the PDS and EIS results (hydrogen evolution measurements also complemented findings from the electrochemical measurements). Of the four inhibitors tested using SVET under defect condition, only quinaldic acid (QDA) displayed improvement compared to the control (SG-No inhibitor) and maintained coating passivity during the 24-h exposure period, with no measured anodic activity outside the defect.	[141]
7	PEO — 8-hydroxyquinoline inhibitor	Mg alloy	3.5 wt.% NaCl	53	0.34	0.086	The obtained experimental results indicate that the protective properties of the samples with inhibitor-containing coating were increased in comparison with the samples without coating (5.3×10^{-5} A/cm^2) and the base coating obtained by plasma electrolytic oxidation method (PEO) (3.4×10^{-7} A/cm^2). The local scanning electrochemical methods of surface investigation, notably Scanning Vibrating Electrode Technique (SVET) and Scanning Ion-Selective Electrode Technique (SIET) were used for determining the kinetics and mechanism of the self-healing	[142]

(*continued on next page*)

Table 5 – (*continued*)

S/N	Coatings systems with inhibitors	Substrate	Corrosive medium	I_{corr} of bare substrate ($\mu A/cm^2$)	I_{corr} of coatings systems ($\mu A/cm^2$)	I_{corr} coatings systems with inhibitor	Remarks/Findings	Reference
							process. The treatment by the solution containing 8-hydroxyquinoline, which inhibits the corrosion process, enables one to increase the protective properties of the composite coating in 30 times in the corrosion-active environment in comparison with the base PEO-coating and avert the intensive destruction of the material.	
8	MgAl-LDH/MBT composite coating	AZ31	3.5 wt.% NaCl	1.39	0.0428	0.0173 (before immersion 0.0782 (after immersion)	The corrosion resistance of the composite coating was evaluated by means of hydrogen evolution measurement, electrochemical impedance spectroscopy (EIS), Tafel polarization curves, and neutral salt spray test. The tests show that the LDH/MBT composite coating has a very low corrosion current density an extremely high charge transfer resistance and does not show any corrosion pits even after 15 days of exposure to a NaCl solution or 7 days of exposure to salt fog environment, manifesting the good and robust corrosion protection.	[143]
9	micro-arc oxidation coating – M–16 inhibitor	AZ31B	3.5 wt.% NaCl	–	–	–	Electrochemical impedance spectroscopy (EIS) and scanning electrochemical microscopy (SECM) are used to study the anti-corrosion performance of the scratched and healed composite coatings immersed in 3.5 wt.% NaCl solution. Results show that the porous MAO coating is suitable to carry inhibitor M–16 and the anti-corrosion performance of the scratched coating is significantly improved by the inhibitor embedded in the MAO coating. The scratched coating exhibits an excellent recovery of the anti-corrosion performance	[144]

							after the heat treatment, which is attributed to the cooperation of dynamic disulfide bonds and shape-memory effect of the self-healing PU coating.	
10	Sol-gel - Paeonia condensation tyrosine (PCTyr) Schiff	ZE21B	0.9 wt.% NaCl	131	4.29	3.64	The biocompatible, self-healing, anti-corrosive sol-gel coating loaded with corrosion inhibitor was fabricated on the Mg substrate through a convenient dip-coating tactic. The corrosion resistance and self-healing ability of the coated samples were evaluated using potentiodynamic polarization method and artificial scratch tests respectively. Results obtained show that the sol-gel coating loaded with PCTyr Schiff base not only did not destroy the stability of the coating but also increased its corrosion resistance. When the coating was damaged, it also showed self-healing ability	[145]
11	Polymeric coating based on polycaprolactone (PCL) – Lawsone inhibitor	AZ31	Hank's solution	3.7	0.53	0.059	Lawsone was incorporated into the coating as a corrosion inhibitor to enhance the passive corrosion protection of the PCL coating through its strong chelation ability of dissolving Mg^{2+}. Anti-corrosion properties of the coatings were assessed by electrochemical techniques and *in vitro* immersion tests. The results obtained demonstrated a remarkable improvement in corrosion resistance of the bare Mg alloy. In addition to the corrosion inhibition effect, incorporation of lawsone provided the coating with a strong antibacterial activity against *Escherichia coli* and *Staphylococcus aureus* bacterial strains. Moreover, the fabricated coating was cytocompatible (viability of > 85%) toward human fetal osteoblast cells. The findings of the study highlighted the great potential of lawsone as a natural corrosion inhibitor for fabrication of corrosion protective,	[146]

(*continued on next page*)

Table 5 – (*continued*)

S/N	Coatings systems with inhibitors	Substrate	Corrosive medium	I_{corr} of bare substrate ($\mu A/cm^2$)	I_{corr} of coatings systems ($\mu A/cm^2$)	I_{corr} coatings systems with inhibitor	Remarks/Findings	Reference
							antibacterial, and biocompatible coatings on Mg-based biodegradable implants.	
12	MgAl Hydrotalcites (HT) coating - 8-quinolinol (8Q) inhibitor	AZ31	3.5 wt.% NaCl	–	5.1	0.82 @ pH 8 0.22 @ pH 9 0.07 @ pH 10 0.67 @ pH 11	8Q-intercalated MgAl HT was fabricated successfully on the AZ31 surface. Anti-corrosion and self-healing properties of the coatings were assessed by electrochemical techniques. The results obtained revealed that the corrosion resistance was significantly improved when the pH of the solution was maintained at 10 with a 0.30 M concentration of 8Q. The hydrophobicity was also introduced to MgAl HT with the intercalation of 8Q, which was retained even after the long immersion. Single-frequency EIS showed the healing on-demand trend due to the chelate formation between 8Q and Mg^{2+}.	[147]
13	Superhydrobobic coatings consisting of Mg silicate nanotubes (MS-TNs) and dodecyltrimethoxysilane (DTMS) -2-mercaptabenzimidazole (2-MBI) inhibitor	AZ31B	3.5 wt.% NaCl	833	8.12×10^{-2}	0.334 (1 day) 0.683 (7 day) 0.996 (14 day) 1.02 (21 day)	The anti-corrosion performances of the dual-function coatings were investigated electrochemical (EIS and PDP) measurements. The results of both electrochemical measurements and the scratch tests demonstrated that, due to the physical barrier function of the superhydrophobic surface and the corrosion-inhibited effect of the MS-TNs(2-MBI) doped layer, the anti-corrosion performance of the AZ31B Mg could be greatly improved by the coating and maintained stably even after 21 days immersion in 3.5 wt.% NaCl solution.	[148]
14	Hybrid - epoxy-silane coating -Ce $(DEHP)_3$ (cerium tri(bis(2-ethylhexyl)phosphate) inhibitor	WE43	0.5 M NaCl	–	–	–	The presence of the inhibitor increased the corrosion resistance, and Electrochemical Impedance Spectroscopy tests carried out in 0.5 M NaCl revealed low frequency impedance modulus (0.01 Hz) around 10 9 Ω cm^2. The pH-dependant self-	[55]

							healing effect of Ce $(DEHP)_3$ was evidenced by localized electrochemical techniques, which revealed inhibition of corrosion propagation in artificial defects and decreased net cathodic current densities compared to an unmodified reference coating. Protective behaviour of Ce $(DEHP)_3$ was related to the combined action of the cerium and organophosphate moieties of this inhibitor, in addition to the protective role of yttrium species derived from the yttrium present in the WE43 Mg alloy. The self-healing ability of the Ce $(DEHP)_3$ -modified coating was evidenced using localized electrochemical techniques (LEIS and SVET). Results obtained showed that Ce $(DEHP)_3$ was able to locally inhibit corrosion activity, preventing the propagation of corrosion activity from the artificial defects.	
15	PEO/Silane/Epoxy coatings with $(Ce(NO_3)_3)$ (inorganic) and 8-Hydroxyquinoline (8-HQ) (organic) inhibitors	AZ31	0.5 wt.% NaCl	–	–	–	The effect of cerium nitrate as an inorganic inhibitor in the PEO layer structure and four organic inhibitors in the silane layer structure for improving the protective and adhesion properties of PEO/Silane/Epoxy coating system was studied. The presence of 8-HQ inhibitor enhanced the protective behavior of the PEO/Silane coating system. According to the EIS results, the presence of inhibitors in the coating systems resulted in the creation of active corrosion protection properties for the coated system through the production of stable precipitations in the PEO coating structure and the complex chelate in the silane layer, so that the highest corrosion resistance was related to the Triplex-Ce-HQ coating system. The active protection behavior of organic and inorganic inhibitors was also confirmed by the EIS test on three-layer coating samples with artificial defects, as well as the EN test. The	[149]

(*continued on next page*)

Table 5 – (*continued*)

S/N	Coatings systems with inhibitors	Substrate	Corrosive medium	I_{corr} of bare substrate ($\mu A/cm^2$)	I_{corr} of coatings systems ($\mu A/cm^2$)	I_{corr} coatings systems with inhibitor	Remarks/Findings	Reference
							presence of amine groups in the silane layer leads to the covalent bonding between the epoxy and silane layers and increased adhesion strength.	
16	Mg–Al LDH with molybdate and lauric acid inhibitors	AZ31	3.5 wt.% NaCl	15.29	0.31	0.0017	Anti-corrosion coatings were fabricated via the *in-situ* growth of the corrosion inhibitors intercalated Mg-aluminum layered double hydroxide (Mg–Al LDH) on AZ31 Mg alloy and then post-sealing it by a super-hydrophobic coating. Potentiodynamic polarization curves and electrochemical impedance spectroscopy were recorded to assess the anti-corrosion performance of prepared coatings. It was found that Mg–Al LDH with molybdate intercalation and lauric acid modification achieves the excellent corrosion inhibition performance (99.99%) due to the multicomponent synergistic effect such as the physical protection of Mg–Al LDH, the corrosion inhibition of molybdate and super-hydrophobic properties of lauric acid.	[150]
17	PEO (Plasma Electrolytic Oxidation)/Sol-gel composite coating with sodium salts of glycolic, 4-aminosalicylic and 2,6-pyridinedicarboxylic acids inhibitors	AZ91	0.5 wt.% NaCl	–	–	–	Three organic Mg corrosion inhibitors, sodium salts of glycolic, 4-aminosalicylic and 2,6-pyridinedicarboxylic acids, were successfully incorporated and immobilized into the porous PEO coating by sealing with a top sol-gel layer. EIS and scanning vibrating electrode technique (SVET) were used to evaluate the corrosion inhibition performance of the coatings. In comparison to the blank coating, all inhibitor-containing composite coatings demonstrated superior corrosion resistance and provided active corrosion protection for Mg alloy AZ91. The active protection	[123]

							mechanism ensures self-healing ability of the coating system, which was obtained by suppression of the re-deposition of impurity and/or adsorption of the impregnated inhibitors upon the exposed surface.	
18	MgAl-LDH coating with thiophene derivative (NTA) inhibitor	AZ31	3.5 wt.% NaCl	5.88	1.54	0.04001	Composite coatings consisting of underlying MgAl-LDH layer and outer films of different CIs were fabricated on AZ31 Mg alloy by a hydrothermal method. Electrochemical tests revealed that the MgAl-LDH film modified with the newly synthesized CI exhibited higher charge transfer resistance and lower corrosion current density than films modified with commercial CIs. The highest enhancement in corrosion resistance was linked to the film's ability to repair physical damage by forming precipitates through chemical complexation and adsorption of the CIs.	[151]
19	Hybrid sol-gel coatings with Alanine, glutamine, and Methionine inhibitors	AZ91	3.5% NaCl	–	–	–	The effect of amino acids on the corrosion resistance of the hybrid MT32 sol-gel coating applied on a pretreated Mg alloy (AZ91) was studied using electrochemical (EIS) technique to improve the protection ability of the coating. The results obtained indicated that among the amino acids used as inhibitors, methionine with the composition of 0.5 wt.% exhibited more enhanced protection properties ($R_{total} = 47\ k\Omega\ cm^2$).	[152]
20	PEO coating with thiourea inhibitor	AZ31	3.5% NaCl	32	0.67	0.08	The synergistic effect on the corrosion protection properties of Mg alloys subjected to plasma electrolytic oxidation and chemically treated with thiourea as an inhibitor was investigated by electrochemical techniques. The addition of thiourea to the inorganic layer substantially increased the corrosion protection performance of the PEO coating. This strategy not only facilitated the formation of a dense, compact coating through thiourea linkages but also	[153]

(*continued on next page*)

Table 5 – (continued)

S/N	Coatings systems with inhibitors	Substrate	Corrosive medium	I_{corr} of bare substrate ($\mu A/cm^2$)	I_{corr} of coatings systems ($\mu A/cm^2$)	I_{corr} coatings systems with inhibitor	Remarks/Findings	Reference
							ensured that the organic inhibitor rectifies the defects and micropores in the PEO coating.	

for this class of metals [31], the inhibitive performance cannot be relied upon. For instance, inhibition efficiency of 64.13% and 58.27%, respectively was reported for hydroxylethyl cellulose and sodium alginate against the corrosion of AZ31 Mg alloy in 3.5 wt.% NaCl solution. alloy. Future researches should thus focus on exploring plant extracts and natural polymers significantly as inhibitor for Mg and its alloys. Suitable intensifiers should also be identified in order to boost the performance of this class of compounds. The realization of green chemistry and the Vision 2030 [154] centered on the utilization of these classes of compounds in chemical production.

3. One of the research interests of the present is the development of lightweight Mg alloys capable of operating at elevated temperatures for possible use in internal combustion engines [155]. Surprisingly, high percentage of research works on the corrosion of Mg and its alloys do not consider the effect on temperature. Most of the investigations are done at low temperatures. Scientists working in this area should consider studying the corrosion of Mg and its alloys at elevated temperatures and developing effective corrosion inhibitors and/or coatings that would make the application of Mg alloys at temperatures as high as >200 °C.

5. Conclusions

The review article takes a look at the inhibition of the corrosion of Mg and its alloys in diverse corrosive media using corrosion inhibitors and coatings containing inhibitors. Mg and its alloys are highly considered because of its light weight for vast industrial applications. The review classified compounds studied as inhibitor for Mg and its alloys into: inorganic, organic (surfactants, ionic liquids, and Schiff bases), hybrid (inorganic-organic), polymeric, and plant extracts. KNO_3 and KCN are highly effective for pure Mg in NaCl solution while Na_2MoO_4 is effective for WE43 alloy. However, their continuous usage is challenged by environmental litigations. The organic, polymeric, and plant extracts in most cases moderately inhibit the corrosion of the alloys. A number of organic compounds have also been seen to accelerate the corrosion of Mg. The review identifies knowledge gaps to include:

i. Scanty information on the use of corrosion inhibitors directly in corrosive solution to protect Mg and its alloys is limited;
ii. Limited information on the natural polymers and plant extracts as corrosion inhibitors for Mg and its alloys; and
iii. Lack of information on the inhibition of Mg and its alloys corrosion in elevated temperatures.

Based on the identified knowledge gaps, it is recommended that future researches should be geared toward filling the existing research gaps.

Declaration of Competing Interest

The authors declare that they have no known competing financial interests or personal relationships that could have appeared to influence the work reported in this paper.

Acknowledgements

The authors gratefully acknowledge the Deanship of Research Coordination and Oversight (DROC) as well as Interdisciplinary Research Center for Advanced Materials (IRC-AM), King Fahd University of Petroleum and Minerals (KFUPM) for support.

REFERENCES

[1] Koch G. In: Trends oil gas corros. res. technol. prod. transm. Elsevier Inc.; 2017. p. 3–30.
[2] Rodríguez-Alonso L, López-Sánchez J, Serrano A, de la Fuente OR, Galván JC, Carmona N. Gels 2022;8:34. 34 8 (2022).
[3] Ouyang Y, Li LX, Xie ZH, Tang L, Wang F, Zhong CJ. J. Magnes. Alloy. 2022;10:836–49.
[4] Jiang Y, Gao S, Liu Y, Huangfu H, Guo X, Zhang J. Surf Coating Technol 2022;440:128504.
[5] Tan B, Lan W, Zhang S, Deng H, Qiang Y, Fu A, et al. Colloids Surfaces A Physicochem. Eng. Asp. 2022;645:128892.
[6] Tan B, Zhang S, Cao X, Fu A, Guo L, Marzouki R, et al. J Colloid Interface Sci 2022;609:838–51.
[7] Cao X, Jahazi M, Immarigeon JP, Wallace W. J Mater Process Technol 2006;171:188–204.
[8] Staiger MP, Pietak AM, Huadmai J, Dias G. Biomaterials 2006;27:1728–34.
[9] Li L, Pan F, Lei J. Magnes. Alloy. - Corros. Surf. Treat. In: Czerwinski F, editor. IntechOpen; 2011.
[10] Atrens A, Shi Z, Mehreen SU, Johnston S, Song GL, Chen X, et al. J. Magnes. Alloy. 2020;8:989–98.
[11] Blawert C, Fechner D, Höche D, Heitmann V, Dietzel W, Kainer KU, et al. Corrosion Sci 2010;52:2452–68.
[12] Williams G, Dafydd HAL, McMurray HN, Birbilis N. Electrochim Acta 2016;219:401–11.
[13] Song GL, Atrens A. Adv Eng Mater 1999;1:11–33.
[14] Song G, Atrens A. Adv Eng Mater 2003;5:837–58.
[15] Song G, Atrens A. Adv Eng Mater 2007;9:177–83.
[16] Atrens A, Dietzel W. Adv Eng Mater 2007;9:292–7.
[17] Petty RL, Davidson AW, Kleinberg J. J Am Chem Soc 2002;76:363–6.
[18] Esmaily M, Svensson JE, Fajardo S, Birbilis N, Frankel GS, Virtanen S, et al. Fundamentals and advances in magnesium alloy corrosion. 2017.
[19] Liu RL, Scully JR, Williams G, Birbilis N. Electrochim Acta 2018;260:184–95.
[20] Heshmati M, Seifzadeh D, Shoghi P, Gholizadeh-Gheshlaghi M. Surf Coating Technol 2017;328:20–9.
[21] Rajabalizadeh Z, Seifzadeh D. Appl Surf Sci 2017;422:696–709.
[22] Xie Z, Yu G, Hu B, Lei X, Li T, Zhang J. Appl Surf Sci 2011;257:5025–31.
[23] Dinodi N, Shetty AN. Corrosion Sci 2014;85:411–27.
[24] Saji VS. J Mater Res Technol 2019;8:5012–35.
[25] Chen XB, Birbilis N, Abbott TB. Corrosion 2011;67:035005. 1.
[26] Chirkunov AA, Zheludkevich ML. Int. J. Corros. Scale Inhib. 2018;7:376–89.
[27] Lamaka SV, Vaghefinazari B, Mei D, Petrauskas RP, Höche D, Zheludkevich ML. Corrosion Sci 2017;128:224–40.
[28] Mei D, Lamaka SV, Feiler C, Zheludkevich ML. Corrosion Sci 2019;153:258–71.
[29] Hu Z, Liu RL, Kairy SK, Li X, Yan H, Birbilis N. Corrosion Sci 2019;149:144–52.
[30] Lei T, Ouyang C, Tang W, Li LF, Zhou LS. Corrosion Sci 2010;52:3504–8.
[31] Umoren SA, Solomon MM, Madhankumar A, Obot IB. Carbohydr Polym 2020;230:115466.
[32] Hsissou R, Benhiba F, Abbout S, Dagdag O, Benkhaya S, Berisha A, et al. Inorg Chem Commun 2020;115:107858.
[33] Hsissou R, Abbout S, Seghiri R, Rehioui M, Berisha A, Erramli H, et al. J Mater Res Technol 2020;9:2691–703.
[34] Montemor MF, Pinto R, Ferreira MGS. Electrochim Acta 2009;54:5179–89.
[35] Peres RN, Cardoso ESF, Montemor MF, de Melo HG, Benedetti AV, Suegama PH. Surf Coating Technol 2016;303:372–84.
[36] Correa PS, Malfatti CF, Azambuja DS. Prog Org Coating 2011;72:739–47.
[37] Mosiałek M, Mordarski G, Nowak P, Simka W, Nawrat G, Hanke M, et al. Surf Coating Technol 2011;206:51–62.
[38] Kouisni L, Azzi M, Zertoubi M, Dalard F, Maximovitch S. Surf Coating Technol 2004;185:58–67.
[39] Kim SJ, Hara M, Ichino R, Okido M, Wada N. Mater Trans 2003;44:782–6.
[40] Song G, StJohn DH. Mater Corros 2005;56:15–23.
[41] Li Y, Ba ZX, Li YL, Ge Y, Zhu XC. Anti-corrosion Methods & Mater 2017;5:486–91.
[42] Li L, Lie L. Surf Technol 2007;36:16–8.
[43] Li J, Hurley B, Buchheit R. J Electrochem Soc 2015;162:563–71.
[44] Feng Z, Hurley B, Li J, Buchheit R. J Electrochem Soc 2018;165:C94–102.
[45] Kartsonakis IA, Stanciu SG, Matei AA, Karaxi EK, Hristu R, Karantonis A, et al. Corrosion Sci 2015;100:194–208.
[46] Lamaka SV, Höche D, Petrauskas RP, Blawert C, Zheludkevich ML. Electrochem Commun 2016;62:5–8.
[47] Zaghloul B, Kish JR. J Electrochem Soc 2021;168:081507.
[48] Ralston KD, Chrisanti S, Young TL, Buchheit RG. J Electrochem Soc 2008;155:C350.
[49] Mahajanam SPV, Buchheit RG. Corrosion 2008;64:230–40.
[50] Birbilis N, Williams G, Gusieva K, Samaniego A, Gibson MA, McMurray HN. Electrochem Commun 2013;34:295–8.
[51] Eaves D, Williams G, McMurray HN. Electrochim Acta 2012;79:1–7.
[52] Williams G, McMurray HN, Grace R. Electrochim Acta 2010;55:7824–33.
[53] Schmutz P, Guillaumin V, Lillard RS, Lillard JA, Frankel GS. J Electrochem Soc 2003;150:B99.
[54] Prince L, Rousseau MA, Noirfalise X, Dangreau L, Coelho LB, Olivier MG. Corrosion Sci 2021;179:109131.
[55] Calado LM, Taryba MG, Morozov Y, Carmezim MJ, Montemor MF. Electrochim Acta 2021;365:137368.
[56] Kharitonov DS, Zimowska M, Ryl J, Zieliński A, Osipenko MA, Adamiec J, et al. Corrosion Sci 2021;190:109664.
[57] Chang Z, Chen X, Peng Y. Miner Eng 2018;121:66–76.
[58] Malik MA, Hashim MA, Nabi F, AL-Thabaiti SA. Int J Electrochem Sci 2011;6:1927–48.
[59] Zhu Y, Free ML, Woollam R, Durnie W. Prog Mater Sci 2017;90:159–223.
[60] Frignani A, Grassi V, Zanotto F, Zucchi F. Corrosion Sci 2012;63:29–39.
[61] Acharya GM, Shetty NA. ChemistrySelect 2021;6:8275–87.

[62] Lu X, Li Y, Ju P, Chen Y, Yang J, Qian K, et al. Corrosion Sci 2019;148:264–71.
[63] Li Y, Lu X, Wu K, Yang L, Zhang T, Wang F. Corrosion Sci 2020;168:108559.
[64] Gao X, Wu Y, Huang Q, Jiang Y, Ma D, Ren T. J Mol Liq 2021;324:114732.
[65] Ramachandran S, Tsai BL, Blanco M, Chen H, Tang Y, Goddard WA. Langmuir 1996;12:6419–28.
[66] Solomon MM, Umoren SA, Quraishi MA, Tripathi D, Abai EJ. J Pet Sci Eng 2020;187:106801.
[67] Zheng Y, Peng R, Jin H, Luo Y, Ping Y. Surf Coating Technol 2017;325:539–47.
[68] Rajendran S. Corros. Prot. Control Using Nanomater. 2012:283–303.
[69] Su H, Liu Y, Gao X, Qian Y, Li W, Ren T, et al. J Alloys Compd 2019;791:681–9.
[70] Jiang Y, Liu Y, Gao S, Guo X, Zhang J. J Mol Liq 2022;345:116998.
[71] Verma C, Quraishi MA. Coord Chem Rev 2021;446:214105.
[72] James Speight PD. Lange's handbook of chemistry. 16th ed. McGraw-Hill Education; 2005.
[73] Ma L, Li W, Zhu S, Wang L, Guan S. Corrosion Sci 2021;184:109268.
[74] Guo Y, Yang S, Feng W, Li Y, Cheng Y. Int J Electrochem Sci 2016;11:6043–51.
[75] Guo X, An M, Yang P, Li H, Su C. J Alloys Compd 2009;482:487–97.
[76] Wang J-L, Ke C, Pohl K, Birbilis N, Chen X-B. J Electrochem Soc 2015;162:C403–11.
[77] Ostanina TN, Rudoi VM, Ovsyannikova AN, Malkov VB. Russ. J. Electrochem. 2010 2010;466 46:707–13.
[78] Su H, Wang L, Wu Y, Zhang Y, Zhang J. Corrosion Sci 2020;165:108410.
[79] Maltseva A, Lamaka SV, Yasakau KA, Mei D, Kurchavov D, Zheludkevich ML, et al. Corrosion Sci 2020;171:108484.
[80] Soltan A, Dargusch MS, Shi Z, Jones F, Wood B, Gerrard D, et al. J. Magnes. Alloy. 2021;9:432–55.
[81] Hu J, Zeng D, Zhang Z, Shi T, Song GL, Guo X. Corrosion Sci 2013;74:35–43.
[82] Dindodi N, Shetty AN. Arab J Chem 2019;12:1277–89.
[83] Papavinasam S. In: Revie RW, editor. Uhlig's corros. handb. 3rd ed. John Wiley & Sons, Ltd; 2011. p. 1021–32.
[84] Zhao Y, Liang P, Shi Y, Wang X. CIE J 2013;64:3714–24.
[85] Lei J, Li L, Yu S, Chen M, Zhang S, Pan F. Chem. Res. Appl. 2008;20:461–4.
[86] Slavcheva E, Schmitt G. Mater Corros 2002;53:647–55.
[87] Hamadi L, Mansouri S, Oulmi K, Kareche A. Egypt. J Petrol 2018;27:1157–65.
[88] Aouniti A, Arrousse N, El-Hajjaji, Salghi R, Taleb M, Kertit S, et al. Arab. J. Chem. Environ. Res. 2017;4:18–30.
[89] Helal NH, Badawy WA. Electrochim Acta 2011;56:6581–7.
[90] Huang D, Tu Y, Huang D, Tu Y, Song G, Guo X. Am J Anal Chem 2013;4:36–8.
[91] Lamaka SV, Montemor MF, Galio AF, Zheludkevich ML, Trindade C, Dick LF, et al. Electrochim Acta 2008;53:4773–83.
[92] Al Zoubi W, Yoon DK, Kim YG, Ko YG. J Colloid Interface Sci 2020;573:31–44.
[93] Al Zoubi W, Yoon DK, Ko YG. J Mol Liq 2020;308:113160.
[94] Al Zoubi W, Ko YG. J Alloys Compd 2019;776:1025–8.
[95] Mohamadian-Kalhor S, Edjlali L, Basharnavaz H, Es'haghi M. J. Mater. Eng. Perform. 2021 2021;301 30:720–6.
[96] Mirzayi B, Basharnavaz H, Babapoor A, Kamali H, Khodayari A, Sohrabnezhad S. Mater Chem Phys 2021;272:125056.
[97] Nashrah N, Putri RAK, Alharissa EZ, Al Zoubi W, Ko YG. Met 2021;11:1043. 1043 11 (2021).
[98] Umoren SA, Solomon MM. Prog Mater Sci 2019;104:380–450.
[99] Umoren SA, Solomon MM, Ali SA, Dafalla HDM. Mater Sci Eng C 2019;100:897–914.
[100] Dang N, Wei YH, Hou LF, Li YG, Guo CL. Mater Corros 2015:1354–62.
[101] Hassan RM, Ibrahim SM, Salman SA, Takagi HD. J. Bio-Tribo-Corrosion 2019 2019;54 5:1–10.
[102] Yang L, Li Y, Qian B, Hou B. J. Magnes. Alloy. 2015;3:47–51.
[103] Da Rocha JC, Da Cunha Ponciano Gomes JA, D'Elia E. Mater Res 2014;17:1581–7.
[104] Muthukrishnan P, Prakash P, Jeyaprabha B, Shankar K. Arab J Chem 2019;12:3345–56.
[105] Alibakhshi E, Ramezanzadeh M, Bahlakeh G, Ramezanzadeh B, Mahdavian M, Motamedi M. J Mol Liq 2018;255:185–98.
[106] Lamia ALA, Oulmas CCO, Dalila BDB, Kadri A, Benbrahim NNB. J. Mater. Process. Environ. 2017;5:18–28.
[107] Halambek J, Berković K, Vorkapić-Furač J. Corrosion Sci 2010;52:3978–83.
[108] Wu Y, Zhang Y, Jiang Y, Qian Y, Guo X, Wang L, et al. J Taiwan Inst Chem Eng 2020;115:35–46.
[109] Wu Y, Zhang Y, Jiang Y, Li N, Zhang Y, Wang L, et al. Colloids Surfaces A Physicochem. Eng. Asp. 2021;626:126969.
[110] Huang D, Hu J, Song GL, Guo X. Electrochim Acta 2011;56:10166–78.
[111] Hu J, Huang D, Zhang G, Song GL, Guo X. Corrosion Sci 2012;63:367–78.
[112] Hu J, Huang D, Song GL, Guo X. Corrosion Sci 2011;53:4093–101.
[113] Barranco V, Carmona N, Galván JC, Grobelny M, Kwiatkowski L, Villegas MA. Prog Org Coating 2010;68:347–55.
[114] Galio AF, Lamaka SV, Zheludkevich ML, Dick LFP, Müller IL, Ferreira MGS. Surf Coating Technol 2010;204:1479–86.
[115] Shi H, Liu F, hou Han E. Prog Org Coating 2009;66:183–91.
[116] Montemor MF, Ferreira MGS. Surf Coating Technol 2008;202:4766–74.
[117] Adsul SH, Sonawane SH, Subasri R. Mater. Perform. Charact. 2022;11.
[118] Anjum MJ, Zhao J, Zahedi Asl V, Yasin G, Wang W, Wei S, et al. Corrosion Sci 2019;157:1–10.
[119] Wang X, Li L, Xie ZH, Yu G. Electrochim Acta 2018;283:1845–57.
[120] Calado LM, Taryba MG, Morozov Y, Carmezim MJ, Montemor MF. Corrosion Sci 2020;170:108648.
[121] Yang J, Blawert C, Lamaka SV, Snihirova D, Lu X, Di S, et al. Corrosion Sci 2018;140:99–110.
[122] Lu X, Blawert C, Tolnai D, Subroto T, Kainer KU, Zhang T, et al. Corrosion Sci 2018;139:395–402.
[123] Chen Y, Lu X, Lamaka SV, Ju P, Blawert C, Zhang T, et al. Appl Surf Sci 2020;504:144462.
[124] Lamaka SV, Knörnschild G, Snihirova DV, Taryba MG, Zheludkevich ML, Ferreira MGS. Electrochim Acta 2009;55:131–41.
[125] Gnedenkov AS, Sinebryukhov SL, Mashtalyar DV, Gnedenkov SV. Corrosion Sci 2016;102:269–78.
[126] Ivanou DK, Yasakau KA, Kallip S, Lisenkov AD, Starykevich M, Lamaka SV, et al. RSC Adv 2016;6:12553–60.
[127] Vaghefinazari B, Wang C, Mercier D, Mei D, Seyeux A, Marcus P, et al. Corrosion Sci 2021;192:109830.
[128] Chen J, Fang L, Wu F, Xie J, Hu J, Jiang B, et al. Prog Org Coating 2019;136:105234.
[129] Song Y, Wang H, Liu Q, Li G, Wang S, Zhu X. Surf Coating Technol 2021;422:127524.
[130] Wu W, Sun X, Zhu CL, Zhang F, Zeng RC, Zou YH, et al. Prog Org Coating 2020;147:105746.
[131] Chen J, Song Y, Shan D, Han EH. Corrosion Sci 2013;74:130–8.

[132] Hou L, Li Y, Sun J, Zhang SH, Wei H, Wei Y. Appl Surf Sci 2019;487:101–8.
[133] Wen T, Yan R, Wang N, Li Y, Chen T, Ma H. Surf Coating Technol 2020;383:125255.
[134] Anjum MJ, Zhao JM, Asl VZ, Malik MU, Yasin G, Khan WQ. Rare Met 2021;40:2254–65.
[135] Li Y, Lu X, Serdechnova M, Blawert C, Zheludkevich ML, Qian K, et al. J. Magnes. Alloy 2021. https://doi.org/10.1016/j.jma.2021.07.015. In press.
[136] Hernández Molina EF, Espinoza Vázquez A, Rodríguez Gómez FJ, Figueroa IA, Negrón Silva GE, Ángeles-Beltrán D. Int J Electrochem Sci 2020;15:10028–39.
[137] Zhang J, Wei J, Li B, Zhao X, Zhang J. J Colloid Interface Sci 2021;594:836–47.
[138] Yan D, Wang Y, Liu J, Song D, Zhang T, Liu J, et al. J Alloys Compd 2020;824:153918.
[139] Li Z, Yu Q, Zhang C, Liu Y, Liang J, Wang D, et al. Surf Coating Technol 2019;357:515–25.
[140] Saei E, Ramezanzadeh B, Amini R, Kalajahi MS. Corrosion Sci 2017;127:186–200.
[141] Upadhyay V, Bergseth Z, Kelly B, Battocchi D. Coatings 2017;7:86.
[142] Gnedenkov AS, Sinebryukhov SL, Mashtalyar DV, Gnedenkov SV. Solid State Phenom 2016;245:89–96.
[143] Hu T, Ouyang Y, Xie ZH, Wu L. J Mater Sci Technol 2021;92:225–35.
[144] Liu S, Li Z, Yu Q, Qi Y, Peng Z, Liang J. Chem Eng J 2021;424:130551.
[145] Li W, Su Y, Ma L, Zhu S, Zheng Y, Guan S. Colloids Surf B Biointerfaces 2021;207:111993.
[146] Asadi H, Suganthan B, Ghalei S, Handa H, Ramasamy RP. Prog Org Coating 2021;153:106157.
[147] Anjum MJ, Zhao J, Tabish M, Murtaza H, Asl VZ, Yang Q, et al. Mater Today Commun 2021;26:101923.
[148] Liu X, He H, Zhang TC, Ouyang L, Zhang YX, Yuan S. Chem Eng J 2021;404:127106.
[149] Toorani M, Aliofkhazraei M, Mahdavian M, Naderi R. Corrosion Sci 2021;178:109065.
[150] Wang X, Jing C, Chen Y, Wang X, Zhao G, Zhang X, et al. J. Magnes. Alloy. 2020;8:291–300.
[151] Li LX, Xie ZH, Fernandez C, Wu L, Cheng D, Jiang XH, et al. Electrochim Acta 2020;330:135186.
[152] Ashassi-Sorkhabi H, Moradi-Alavian S, Jafari R, Kazempour A, Asghari E. Mater Chem Phys 2019;225:298–308.
[153] Al Zoubi W, Ko YG. Sci. Rep. 2018;81(8):1–11 (2018).
[154] Lerner S. Europeans Aim to Phase Out Toxic PFAS Chemicals by 2030. The Intercept. 2019. https://theintercept.com/2019/12/19/pfas-chemicals-europe-phase-out/. [Accessed 6 October 2020].
[155] Dong X, Feng L, Wang S, Nyberg EA, Ji S, Magnes J. Alloy 2021;9:90–101.

Dr. Saviour A. Umoren is a Professor/ Senior Research Scientist at the Interdisciplinary Research Center for Advanced Materials (IRC-AM), King Fahd University of Petroleum & Minerals (KFUPM), Dhahran, Saudi Arabia. He obtained his BSc in Applied Chemistry from the University of Jos, Nigeria in 1990 and MSc in Polymer Science and Engineering and PhD in Polymer Science from the Federal University of Technology, Owerri, Nigeria in 1997 and 2008 respectively. He was a Postdoctoral Research Fellow at the State Key Laboratory for Corrosion and Protection, Institute of Metal Research, Chinese Academy of Sciences, Shenyang, China courtesy of TWAS – CAS Postdoctoral Research Fellowship award from May 2009–April 2010 and a visiting researcher at Research Institute of Theoretical and Applied Physical Chemistry (INIFTA), La Plata, Argentina courtesy of TWAS – UNESCO Associateship appointment. He has authored/co-authored over 150 research articles in international peer reviewed journal mostly ISI rated including several critical reviews and some of his publications have been highly cited. He has 3 granted US Patents, one authored (Polymeric Materials in Corrosion Inhibition: Fundamentals and Applications, Elsevier, 2022) and one edited (Corrosion Inhibitors for the Oil and Gas Industry, Wiley, 2020) books and many book chapters to his credit. He is an Associate Editor of Frontiers in Materials, Polymer and Composite Materials section and Petroleum Research (Elsevier) as well as editorial board member of twelve (12) international journals. He has also served as a reviewer to more than one hundred and fifty (150) international journals. His research interests is extensively on investigation of corrosion and corrosion inhibition phenomena in different environments. His current research is on polymer composites/nanocomposites for corrosion protection and environmentally friendly corrosion inhibitors development for industrial metals. He is a member of a number of professional Associations including International Society of Electrochemistry (ISE), National Association of Corrosion Engineers (NACE), American Chemical Society (ACS), Royal Society of Chemistry (RSC) and Chemical Society of Nigeria (CSN) amongst others.

Mr. Mohammed T. Abdullahi obtained a BSc in Chemistry (First Class, Honours) from Usman Dan Fodio University Sokoto, Nigeria in 2014 and MSc in Chemistry from King Fahd University of Petroleum and Minerals (KFUPM) in 2020. Currently, he is a PhD student in the Department of Chemistry, KFUPM, Dhahran, Saudi Arabia. Prior to resuming graduate studies at KFUPM, he was a Chemistry lecturer at the College of Education Zuba, Abuja, Nigeria. His research research interest is on the development of novel materials for several applications.

Dr. Moses M. Solomon is a Senior Lecturer at the Department of Chemistry, College of Science and Technology, Covenant University, Ota, Nigeria. He obtained a PhD in Polymer Chemistry from University of Uyo, Nigeria in 2016. He was a postdoctoral research fellow at Duzce University, Turkey (2016–2017) and at the Interdisciplinary Research Center for Advanced Materials, KFUPM, Saudi Arabia (2018–2020). He is a seasoned material and corrosion scientist with internationally recognized teaching and research skills. Research is focused on organic synthesis, characterization, modification, and extensively on investigating materials corrosion and corrosion inhibition mechanisms on conventional polycrystalline as well as nanocrystalline surfaces. Dr Solomon has published 85 journal articles, 10 book/book chapters, and 10 conference papers. He has 2 granted patents (1 US and 1 Turkish) and other invention disclosures to his credit. He is the co-author of the most-rated review article on corrosion inhibition published in Progress in Material Sciences with Impact Factor of 48.165. His SCOPUS h-index is 33, Field-Weighted Citation Impact of 2.47, and total citation of 3341. In Google Scholars, he has a h-index of 35 and total citation of 4158.